Towards a new lumped parameterization at catchment scale

R.G. Benning

RAPPORT 54

Februari 1995

Vakgroep Waterhuishouding
Nieuwe Kanaal 11, 6709 PA Wageningen

ISSN 0926-230X

Doctoral thesis performed at
University of Bologna, Italy, department of hydraulic construction
under supervision of
Prof. Ing. E. Todini (It.) and Prof. Dr. Ing. J.J. Bogardi (Nl.)
and assisted by Dott. Ing. P. Di Giammarco (It.)

February 1994

FOREWORD

Along the European integration process a medieval custom has been reinvented. Instead of apprentices wandering from guild to guild now students roam the continent to accomplish their academic and professional forming at an other university than their alma mater.

Ir. Roland Benning was one of the participating students, who benefitted from the existence of the Interuniversity Cooperation Programme in Hydrology and Water Management within the framework of the ERASMUS Programme of the European Union. He spent several months in Bologna to prepare this thesis. The result of his "mobility" - to use the European terminus technicus for this exchange programme - is not only an excellent piece of work, but also the accomplishment of a bit of European integration.

Therefore my thanks as representative of the home university go beyond the appreciation of the academic supervision of Mr. Benning's hosts. Prof. Ezio Todini of the University of Bologna and his collaborators, especially Dr. P. Di Giammarco deserve the credit both academically and for their contribution towards European unity.

Prof. Dr.-Ing. J.J. Bogardi,
Chairman Department of Water Resources

Wageningen, February 1995

ABSTRACT

Ever since the beginning of rainfall-runoff modelling hydrologists have tried to create physically based models with structural simplicity. Runoff produced by rainfall intensities in excess of soil infiltration capacity (Horton excess) and runoff produced by rain falling on saturated soil zones (saturation excess) together with subsurface storm flow are considered in different models to describe the process of runoff.
In 1979, Beven and Kirkby developed TOPMODEL, a hydrological forecasting model combining, a dynamic contributing area model based on $\ln(a/\tan\beta)$ (the topographic index), the channel network topology, and a simple lumped parameter basin routing model.. The predominant factors determining the formation of runoff in this model is represented by the topography of the basin and a negative law linking the transmissivity of the soil with the distance of the saturated zone below ground level.
An extensive analysis of this TOPMODEL has been performed which revealed a number of problems related to its physical interpretation.

The first one is the dependency of the permeability parameter on the grid scale, mainly originated by the steady state assumption which neglects the transient phase, the duration of which depends on the grid size. The second one relates to the difficulty in preserving the water balance within the soil column. This is also originated by the extremely high values of the permeability (a consequence of its dependency on the horizontal grid scale), which reduces the amount of water available for evapotranspiration in the unsaturated zone.

In order to improve the physical interpretation of a topographic based model in general, this doctoral thesis reaches an alternative analytical solution for flow in the downslope direction. This analytical approach formulates a kinematic horizontal flow problem, based on a horizontal transmissivity that can be expressed as a function of the integral vertical moisture content. It shows that the expression used for the dependency of the transmissivity on the total water content in the vertical column follows more or less the same law adopted for the dependency of the permeability on the local water content as described by Brooks and Corey (1964) and van Genuchten (1980).

Although some approximations have been made about the variation of reduced moisture content with depth, this new approach gives good results and can therefore be used as an alternative for describing the physical process of runoff in the unsaturated zone in the TOPMODEL as well as in other topographical based rainfall-runoff models.

TABLE OF CONTENTS

1. INTRODUCTION

The dominant mechanisms in the generation of streamflow are overland flow, saturated and unsaturated subsurface flow and deep aquifer flow (Freeze, 1972a,b; Smith and Hebbert, 1983).
Overland flow may occur because of saturation from above (Hortonian excess), because of saturation from below (saturation excess) or when subsurface flow is forced up to the surface by the soil or slope configuration (return flow). Hortonian overland flow occurs on soils exhibiting low infiltration capabilities, such as on agricultural land, unvegetated surfaces and in desert and urban areas. It is however very rare to occur in steeply sloping catchments in humid vegetated areas. Overland flow due to saturation from below is in these catchments the primary mechanism at work (Freeze, 1972b; Sloan and Moore, 1984).
Subsurface flow is likely to be significant in catchments with soils having high hydraulic conductivity's and an impermeable or semi permeable layer at shallow depth that can support a perched water table. Such conditions often occur in humid vegetated catchments where the organic litter protects the mineral soil and maintains high surface permeability's. This upper soil profile is often interlaced with macropores caused by roots, decayed root holes, worm holes and other structural channels. When percolating water moving vertically in such a medium reaches an impermeable layer, lateral subsurface flow is generated (Beven and Germann, 1982). Under such conditions water movement occurs in two domains: through the micropores (i.e. the saturated soil matrix) and through the interconnected macropores of the soil system (unsaturated conditions). Where a significant portion of the total flow takes place in the macropores, the response time of subsurface flow to rainfall approaches that of overland flow, giving rise to a high perceived hydraulic conductivity for the soil profile as a whole (Whipkey, 1965; Mosley, 1979). The response time of flow within the soil matrix is much slower, and except under special conditions such flow may provide only a small contribution to the total storm flow response of a catchment (Sloan and Moore, 1984).
The last mentioned deep aquifer flows give no significant response on a storm event. The response time caused by the vertical transport of water through the thick soil above this aquifer is so large that we can speak of a constant horizontal flow in this aquifer with no significant response on one specific storm event in a catchment.

This report will concentrate on the rainfall-runoff processes in hilly humid vegetated catchments, with emphasis on the subsurface flow in both theory and modelling. Currently, a lot of models exist to predict hillslope flow using various assumptions, including the following:

(1) Saturated subsurface flow only, using Boussinesq theory (Zecharias and Brutsaert, 1988) or using the kinematic wave assumption (Henderson and Wooding, 1964; Beven, 1981).
(2) Empirical relations (Soil Conservation Service, 1972).
(3) Saturated and unsaturated subsurface flow, using Richard's equation (Nieber and Walter, 1981) or using the kinematic wave assumption (Beven, 1982; Sloan and Moore, 1984; Hurley and Pantelis, 1985; Stagnitti et al. 1986; Steenhuis et al., 1988).

The model presented in this paper is based on the last mentioned category, using the kinematic wave theory and simplifications for hydraulic conductivity with moisture content.

The literature contains many works that summarise the level of understanding of the physics of the complex problem of rainfall-runoff transformation (Dunne, 1978, Freeze, 1980). Many efforts have been made to schematise the whole process in order to develop mathematical models (Dooge, 1957, 1973, Amorocho and Hurt, 1964, Freeze and Harlan, 1969, Todini, 1989). This ranges from the simple calculation of design discharge to the two-dimensional representation of the various processes based on suitably and reciprocally conditioned mass balance, energy and momentum equations (SHE, Abbot et al. 1986a,b, Bathurst, 1986, IHDM, Beven et al, 1987), and to the three-dimensional representation of all the exchanges (Binley et al., 1989). Taken together, these latter kinds of model comprise the broad category of distributed differential models (Todini, 1988); they are frequently referred to as "physical models" to highlight the fact that their respective parameters are (or should be) reflected in the field measurements (Beven, 1989). Given their nature, they are mainly used in investigations and research as a mathematical support for the interpretation of physical reality. The last decade however there has been a demand for models that are simple in terms of calibration and validation and with only a few parameters, corresponding with reality, to describe the physical process.

The TOPMODEL (Beven and Kirkby, 1979, Sivapalan et al., 1987) is one of this latter models and is subject of research in this paper. TOPMODEL is a hydrological forecasting model combining, a dynamic contributing area model based on $\ln(a/\tan\beta)$ (the topographic index), the channel network topology, and a simple lumped parameter basin routing model.. The predominant factors determining the formation of runoff in this model is represented by the topography of the basin and a negative law linking the transmissivity of the soil with the distance of the saturated zone below ground level. The model is characterised by only three parameters and an index curve taken from the DTM (Digital Terrain Map) that describes the topography of the catchment.
The total flow is calculated as the sum of two terms: surface runoff and flow in the saturated zone. The surface runoff, in the most recent versions of the model, is in turn the sum of two components, the first generated by infiltration excess (Horton mechanism) and the second, referring to a variable contributing area, by saturation excess (Dunne mechanism). All the water available for flow is derived from the soil in saturated conditions. In TOPMODEL the unsaturated part of the soil is not considered to produce downslope flow.

Though a synthetic model, i.e. one in which the physical reality is represented in a simplified way, the TOPMODEL is frequently described as being "physically based", in the sense that "the model parameters are physically based in the sense that they may be determined directly by measurement" (Beven and Kirkby, 1979, Sivapalan et al., 1987). This definition is somewhat optimistic in view of the mathematical description of subsurface flow and the resulting unrealistic high outcome for hydraulic conductivity by use of increasing grid size. This paper gives, by a fundamental analysis of the TOPMODEL and the theory representing the saturated and unsaturated subsurface

flow, a simplified kinematic solution that can be applied in the TOPMODEL. In order to make it a more physically bases model in the sense that the parameters are conformable with real values.

Two components can be identified in all conceptual rainfall-runoff models; the first represents the water balance at soil level and the second the transfer to the basin outlet. The water balance at the soil level is the component that characterises the model and constitutes the most important part. Cordova and Rodriguez-Iturbe (1983) summarise this concept most succinctly, saying "... the problem is not *what* to route than *how* to route". This report gives an analytical solution of the last mentioned problem.

Now that the scope of this report is introduced an overview will be given of the line of research followed. We begin with a short overview of the history of rainfall-runoff modelling in chapter 2. In order to get a better understanding of the physical processes involved in the TOPMODEL chapter 3 describes the most important once, systematically. In chapter 4 the version of Franchini et al. (1993) of TOPMODEL is presented and analysed and on some points compared with the version of Sivapalan et al. (1987). The imperfections of the TOPMODEL and a discussion about alternative solutions are given in chapter 5 as well as the introduction of an analytical solution. Chapter 6 gives the kinematic wave solution and the hydraulic conductivity related with moisture content as alternative applications for the TOPMODEL and gives results of comparisons made of different approaches. Finally the conclusions will be reported in chapter 7.

2. A REVIEW OF RAINFALL-RUNOFF MODELLING

The origins of rainfall-runoff modelling in the broad sense can be found in the second half of the 19th century, arising in response to three types of engineering problems: urban sewer design, land reclamation drainage systems design and reservoir spillway design. In all these cases the design discharge was the major parameter of interest.
According to Dooge (1957, 1973), at the end of the nineteenth and the beginning of the twentieth century most engineers either used empirical formulas, derived from specific cases and applied to other cases under the assumption that conditions were similar enough, or they used the "rational method", which may be regarded as the first attempt to approach rationally the problem of predicting runoff from rainfall.
The method, which was derived for small or mountainous catchments was based upon the concept of concentration time. The maximum discharge, caused by a given rainfall intensity, happens when rainfall duration equals or is larger than the concentration time, i.e. the time that the drop of water which falls further away from the closure section takes to reach this section.

During the nineteen twenties, when the need for a corresponding formula for larger catchments was perceived, many modifications were introduces in the rational method in order to cope with the non uniform distribution, in space and time, of rainfall and catchment characteristics.
The modified rational method, based on the concept of isochrones, or lines of equal travel time, can be seen as the first basic rainfall-runoff model based on a transfer function. The shape and parameters were derived by means of topographic maps and the use of Mannings formula, which describes the resistance to flow because of roughness, to evaluate the different travel times. The types of problems to be solved were much the same as before, but hydrologists were trying to provide more realistic and accurate solutions, although still in terms of surface runoff.

In 1933 Sherman introduced the concept of the unit hydrograph on the basis of the superposition principle (Todini, 1989). Although not yet known at the time, the superposition principle implied many assumptions, i.e. the catchment behaves like a causative, linear time invariant system with respect to the rainfall/surface runoff transformation. The unit hydrograph principle accelerated the interest of hydrologists who were now in a position to produce estimates, not only of the peak discharge, but also of the hydrograph caused by more complex storms. Yet the unit hydrograph method presented a certain number of problems which were solved using more or less subjective methods:

- separation of surface runoff from base flow;
- determination of "effective" rainfall, namely that portion of the rainfall that is not lost by evaporation and transpiration and does not filter down through the soil;
- the actual derivation of the unit hydrograph from the available data.

Solutions to all these problems involved an extremely high degree of subjectivity.

At the end of the thirties and during the forties a number of techniques were proposed in order to improve the objectivity of methods and results, and the techniques of statistical analysis were invoked. A discussion on the different approaches and the relevant bibliography can be found in a report by Dooge (1973).

The real breakthrough came in the fifties when hydrologists became aware of system engineering approaches used for the analysis of complex dynamic systems. They finally realised that the unit hydrograph was the solution of a causative, linear time invariant system and that the use of mathematical techniques such as Z, Laplace or Fourier transforms could lead to the derivation of the response function from the analysis of input and output data. The derivation of the unit graph from sampled data (known as the inverse problem) still remained a big problem, due to the non particularly linear behaviour of the system and the generally large errors in input and output data.
To overcome this problem, hydrologists found that shapes of the unit hydrograph could be provided on the basis of the solution of more or less simplified differential equations, such as for instance those describing the time behaviour of the storage in a reservoir or in a cascade of reservoirs (Nash, 1958).

In the sixties other approaches to rainfall-runoff modelling were considered. In search for a more physical interpretation of the process one could represent the behaviour of single components of the hydrological cycle, at the catchment scale, by using a number of interconnected conceptual elements, each of which represented the response of a particular subsystem. The need for such an approach arose from the following requirements:

(1) to extend the use of the model to long continuous records;
(2) to apply the model to complex watersheds with a large variety of soils, vegetation, slopes, etc.; and
(3) to extend the model more or less without calibration to other similar catchments.

A number of these models appeared: Dawdy-O'Donnel (1965), the Stanford Watershed Model IV (Crawford and Linsley, 1966), the Sacramento (Burnash et al., 1973), the SSARR (Rocwood and Nelson, 1966) and the Tank (WMO, 1975). They represented differently the interconnected subsystems and were considered the "top models" of the sixties.

In theory, if the structural description was correct the parameters of the model, such as storage (surface, saturated unsaturated zones), friction factors and threshold effects could be related to the actual physics of the catchment. Unfortunately, in many cases, the large number of parameters used in the models and the fact that these were calibrated in a "best fit" basis, lead to sets of unrealistic parameter values, generally incorporating errors in data and moreover errors in the basic description of the interrelations between simple process models.
This lake of a one-to-one relationship between model and reality gave rise to produce a model which would integrate the partial differential equations expressing the continuity of mass and momentum and linking the sub process models by matching the relevant boundary conditions. The product of such an effort is the "SHE" (Système Hydrologique

Européen) (Abbot et al., 1986a,b). SHE allows the simulation of the internal as well as external effects of catchment behaviour.

The seventies saw a growing awareness and concern for soil erosion and degradation problems, pollutants diffusion, and in general of the environmental impact of anthropological influences on land use changes.
Another type of rainfall-runoff model was developed in the late seventies and in the eighties: the real-time forecasting model as an answer for the need of warnings in flood prone areas, and as a tool for reservoirs or hydraulic structures management. Generally based on recent updating and re calibrating techniques, real-time forecasting models must be reliable, up datable and constitute part of an entire forecasting system which must include automatic real-time data acquisition, data validation, forecasting procedures and produce results in a simple and readily understood form (Bacchi et al. 1986).
Beven en Kirkby (1979) were among the first to work on this area. They employed topographic index methods to predict variable contributing areas. The topographic index, $\ln(a/\tan\beta)$, where "a" is the area drained per unit contour length and "tan β" is the slope of the ground surface at the location , has been found by Beven en Kirkby to compare favourably with observed patterns of surface saturation.

The TOPMODEL (TOPographical MODEL) with was developed in England by K. Beven and M.J. Kirkby (Beven and Kirkby, 1979; Sivapalan et al., 1987), is an example of the last mentioned models. The TOPMODEL is a simple physically based conceptual model in which the predominant factors determining the formation of runoff are represented by the topography of the basin and a negative law linking the transmissivity of the soil with the distance of the saturated zone below ground level. The model can be considered as a presentation of the level of modelling hydrologists have reached until now. This paper tries, after a profound analyse of the TOPMODEL and its theory, to give a modification of the description of the runoff process in the unsaturated zone with the aim to improve the physical meaning of the model. Before going to the TOPMODEL however, some basic physical processes that are described in TOPMODEL will be discussed in the next chapter.

3. PHYSICAL PROCESSES

This chapter will give a summation of the physical processes concerning rainfall-runoff models and used terminology in the literature to give a better understanding of the description of TOPMODEL given in chapter 4.

3.1 The hillslope hydrological cycle

It is exceptional for as much as 5 per cent of catchment rainfall to fall directly on channels and lakes. The remainder reaches channels by the hillslopes; or is lost upwards through evapotranspiration, or downwards to deep aquifers. In appendix 1 we see the complex three-dimensional mosaic of soils, vegetation and bedrock of a hillslope, which is difficult to sample adequately. The exact understanding of the detailed processes acting within a uniform element of soil remains incomplete. The cost and time involved in applying such detailed knowledge for even a small catchment is likely to remain prohibitive for most applications. Hillslope hydrology has therefore been dominated by attempts to simplify, using many assumptions, the processes enough to construct models (see chapter 2). The main components into which precipitation may be partitioned are evapotranspiration, overland flow and saturated and unsaturated subsurface flow.
To give a correct understanding of the terminology concerning the runoff process, used in this paper the following definitions are given in consonance with the article of Freeze 1972b, in the next subparagraph.

3.1.1 Definitions of runoff

Runoff is that part of the precipitation that appears as streamflow either in perennial or intermittent form. It is the flow collected from a drainage basin that appears at the outlet of the basin. *Surface runoff* is that part of the runoff that travels over the surface of the ground to reach a stream channel and through the channel to reach the basin outlet. *Subsurface runoff* is that part of the runoff that travels through the ground to reach a stream channel and through the channel to reach the basin outlet.
The flow at the downstream end of any reach of channel is termed the *channel flow (streamflow)*. Channel flow is the sum of the channel flow to the reach, the lateral inflow along the reach, and the channel precipitation along the reach.
According to the source from which it is derived the lateral inflow may consist of *overland flow*, *subsurface flow* and *base flow*. *Overland flow* is that part of the lateral inflow that flows over the land surface toward a stream channel. *Subsurface storm flow* (interflow, through flow) is that part of the lateral inflow derives from water that infiltrates the soil surface and moves laterally through the upper soil horizons toward the stream channels as unsaturated flow or shallow perched saturated flow above the main groundwater level. *Base flow* is that part of the lateral inflow derived from deep percolation of infiltrated

water that enters the permanent saturated groundwater flow system and discharges into the stream channel.

Total subsurface flow is the sum of the base flow and subsurface storm flow, and is equal to the total flow of water arriving at the stream as saturated flow into the stream bed itself, and as percolation from the seepage faces on the stream bank. Subsurface storm flow that discharges into the transient, near-channel wetlands that develop during storm periods is probably best considered as part of the total subsurface flow. When such discharge occurs at a distance from the main channel it commonly does so at fixed points of seepage in topographic lows. Sometimes this outflow might be considered as a contribution to overland flow, but more usually it feeds its own intermittent tributary channel for which all the definitions given above apply.

3.1.2 Mechanisms of runoff production

Runoff in actual catchments is produced by a number of different mechanisms. Appendix 2 shows a spectrum of processes that may be involved in flood runoff production. According to Dunne (1978), the primary sources of runoff produced on hillslopes during storm runoff events is overland flow. Overland flow is produced at any location in a catchment due to the surface soil layers being saturated. In the model under study, the total flow is calculated as the sum of two terms: surface runoff and flow in the saturated zone. The surface runoff, in the most recent versions of the TOPMODEL, is in turn the sum of two components, the first generated by infiltration excess (Horton mechanism) and the second, referring to a variable contributing area, by saturation excess (Dunne mechanism).

The first mechanism, first espoused by Horton (1933), is for a rainfall intensity that exceeds the saturated hydraulic conductivity of the soil. The moisture content at the surface increases as a function of time and, at some point in time, the surface becomes saturated and an inverted zone of saturation begins to propagate downward into the soil. At this time the infiltration rate drops below the rainfall rate and overland flow is produced. As originally presented, Horton's infiltration excess mechanism inferred that most rainfall events exceed infiltration capacities and that overland flow is common and spatial widespread. But in general only a part of a catchment contributes to overland flow (see appendix 1). A great heterogeneity in soil types over a catchment and the very irregular patterns of rainfall in time and space creates a very complex hydrologic response at the land surface. The infiltration excess (Horton) mechanism tends to dominate overland flow production in most desert or semiarid regions, where the absence of vegetation and other organic matter prevent the development of a porous soil structure through which water can move easily. On vegetated surfaces in humid regions however, Hortonian overland flow occurs rarely (Dunne et al., 1975).

The second mechanism of surface runoff production occurs where the soil becomes saturated to the surface from below due to both rainfall inputs and downslope

subsurface flow. This saturation excess (Dunne) mechanism is most common on near-channel wetlands. The area of saturation will expand and contract during and between storms. The Dunne mechanism can result in surface runoff production in humid and vegetated areas with shallow water tables, even where infiltration capacities of the soil surface are high relative to normal rainfall intensities. The main controls on the saturated contributing areas are the topographic and hydrogeologic characteristics of the hillslopes.

The literature also reports a third mechanism of overland flow which is called return flow (Kirkby, 1985). This process can even occur after rainfall has ceased where subsurface flow is forced up to the surface by the soil or slope configuration. The return flow occurs usually on concave slope profiles and areas of flow convergence. For the sake of simplicity of many rainfall-runoff models (as also the TOPMODEL), this process of overland flow is mostly neglected.

3.2 Infiltration

Infiltration is the process of water penetrating from the ground surface into the soil. Many factors influence the infiltration rate, including the condition of the soil surface and its vegetative cover, the properties of the soil, such as its porosity and hydraulic conductivity, and the current moisture content of the soil. Infiltration is a very complex process that can be described only approximately with mathematical equations (Chow et al., 1988).

3.2.1 Continuity equation

The continuity or storage equation for one-dimensional unsteady unsaturated vertical flow in a porous medium is:

$$(3.1) \quad \frac{\partial \theta}{\partial t} + \frac{\partial q}{\partial z} = 0$$

where: θ = soil moisture content defined as $\theta = \frac{volume\ of\ water}{total\ volume}$

t = time
q = Darcy flux, $q = Q/A$
z = z axis (vertical one)

This equation is applicable to vertical flow at shallow depths below the land surface. At greater depth, such as in deep aquifers, changes in the water density and in the porosity can occur as the result of changes in fluid pressure, and these must also be accounted for in developing the continuity equation.

3.2.2 Richard's equation (momentum equation)

Darcy's law for flow in a porous medium can be written as:

(3.2) $q = KS_f$

where q is the Darcy flux, K is hydraulic conductivity and S_f is the friction slope. Consider flow in the vertical direction and denote the total head of the flow by h; then $S_f = -\partial h / \partial z$ where the negative sign indicates that the total head is decreasing in the direction of flow because of friction. Darcy's law is then expressed as:

(3.3) $$q = -K\frac{\partial h}{\partial z}$$

The total head h is the sum of the suction and gravity heads

(3.4) $h = \psi + z$

where: ψ = suction head
z = gravity head

No term is included for the velocity head of the flow because the velocity is so small that its head is negligible.
Substituting for h in equation (3.3):

(3.4) $$q = -K\frac{\partial(\psi + z)}{\partial z}$$

$$= -\left(K\frac{d\psi}{\partial\theta}\frac{\partial\theta}{\partial z} + K\right)$$

$$= -\left(D\frac{\partial\theta}{\partial z} + K\right)$$

where D is the soil water diffusivity $K(d\psi / d\theta)$ that has dimensions $\left[L^2 / T\right]$. Substituting this result into the continuity equation (3.1) gives:

(3.5) $$\frac{\partial\theta}{\partial t} = \frac{\partial}{\partial z}\left(D\frac{\partial\theta}{\partial z} + K\right)$$

which is a one-dimensional form of Richard's equation, the governing equation for unsteady unsaturated vertical flow in a porous medium, first presented by Richards (1931).

3.2.3 Horton's equation

One of the earliest infiltration equations was developed by Horton (1933, 1939), who observed that infiltration begins at some rate f_0 and exponentially decreases until it reaches a constant rate f_c (see Appendix 3):

$$(3.6) \quad f(t) = f_c + (f_0 - f_c)e^{-kt}$$

where k is a decay constant having dimensions $[T^{-1}]$. Eagleson (1970) and Raudkivi (1979) have shown that Horton's equation can be derived from Richard's equation (3.5) by assuming that K (hydraulic conductivity) and D (soil water diffusivity $K(d\psi / d\theta)$) are constants independent of the moisture content of the soil. Under these conditions (3.5) reduce to:

$$(3.7) \quad \frac{\partial \theta}{\partial t} = D\frac{\partial^2 \theta}{\partial z^2}$$

which is the standard form of a diffusion equation and may be solved to yield the moisture content θ as a function of time and depth. Horton's equation results from solving for the rate of moisture diffusion $D(\partial\theta / \partial z)$at the soil surface.

3.2.4 Philip's equation

Philip (1957) solved Richard's equation under less restrictive conditions by assuming that K and D can vary with the moisture content θ . Philip employed the Boltzmann transformation $B(\theta) = zt^{-1/2}$ to convert equation (3.5) into an ordinary differential equation in B, and solved this equation to yield an infinite series for cumulative infiltration $F(t)$, which is approximated by:

$$(3.8) \quad F(t) = St^{1/2} + Kt$$

where S is a parameter called sorptivity, which is a function of the soil suction potential, and K is the hydraulic conductivity.
By differentiation:

$$(3.9) \quad f(t) = \frac{1}{2} S t^{-1/2} + K$$

As $t \to \infty$, $f(t)$ tends to K. The two terms in Philip's equation represent the effects of soil suction head and gravity head, respectively. For a horizontal column of soil, soil suction is the only force drawing water into the column, and Philip's equation reduces to $F(t) = St^{1/2}$.

3.2.5 Green-Ampt method

In the previous two subparagraphs, infiltration equations were developed from approximate solutions of Richard's equation. An alternative approach is to develop a more approximate physical theory that has an exact analytical solution. Green and Ampt (1911) proposed the simplified picture of infiltration shown in appendix 4. The wetting front is a sharp boundary dividing soil of moisture content θ_i below from saturated soil with moisture content η above. The wetting front has penetrated to a depth L in time t since infiltration began. Water is pounded to a small depth h_0 on the soil surface. For the exact derivations that lead to the analytical solution we refer to Chow et al., 1988. The Green-Ampt equation for cumulative infiltration is:

$$(3.10) \quad F(t) = Kt + \psi \, \Delta\theta \, \ln\left(1 + \frac{F(t)}{\psi \, \Delta\theta}\right)$$

where: $\Delta\theta = \eta - \theta_i$

θ_i = moisture content in initial condition
η = porosity
ψ = suction head
K = hydraulic conductivity

The F is to be found by the successive substitution method. Given K, T, ψ and $\Delta\theta$, a trail value F is substituted on the right-hand side (a good trial value is $F = Kt$), and a new value of F calculated on the left-hand side, which is substituted as a trial value on the right-hand side, and so on, until the calculated values of F converge to a constant. The final value of cumulative infiltration F is substituted into the following equation:

$$(3.11) \quad f(t) = K\left(\frac{\psi \, \Delta\theta}{F(t)} + 1\right)$$

to determine the corresponding potential infiltration rate f.

3.3 Saturated subsurface flow

A crucial role for any saturated flow model is the estimation of the "saturated contributing area" and its variations during a storm. Under the simple conditions of indefinite steady rainfall excess (appendix 5) the level of saturation in the soil may be estimated as follows. For an area of a, draining into a one-metre contour width, the steady-state discharge to balance rainfall excess is:

(3.12) $q = ia$

where "i" is the intensity of steady rainfall excess with dimension's mm/hr.
This discharge may also be related to hydraulic gradient and Darcian flow within the permeable soil. If the water table is assumed to parallel the soil surface then hydraulic gradient is equal to topographic gradient and the discharge may also be expressed as:

(3.13) $q = q_0 \phi(D) s$

where D = the soil moisture total deficit below saturation;

q_0 = the soil discharge at saturation on unit hydraulic gradient at the outflow point;

$\phi(D)$ = the ratio of flow at deficit D to the flow at saturation; and

s = the local gradient at the outflow point.

Combining equations (3.12) and (3.13) gives:

(3.14) $$\phi(D) = \frac{i}{q_0} . \frac{a}{s}$$

Since ϕ is inevitably a decreasing function, deficit must decrease as rainfall intensity increases and also responds predictably to local topography (a/s) and soil (q_0). Thus deficit is small (or the soil wet) in areas of thin or impermeable soils (low q_0), in hollows (high a) or on low gradients (low s). On a typical convex-concave profile, deficit remains roughly constant across the convexity (a x s) and then decreases steadily on the concavity (a increasing and s decreasing). In particular, saturated conditions are reached where
$\phi(D) = 1$ or $a/s = q_0/i$.
These expressions are not appropriate for estimation of storm flow, but can be used as an approximation for antecedent conditions at the beginning of a storm. During a storm, saturated flow may be obtained as the kinematic wave solution (see chapter 6) of the continuity equation, subject to the flow law of equation (3.13):

$$(3.15)\quad \frac{1}{w}\frac{\partial (wq)}{\partial x} - \frac{\partial D}{\partial t} = i$$

where w is the width of the catchment element at distance x (measured along the flow lines, see appendix 5) from the divide, and i is the net input to the saturated zone. This input should be delayed to allow for unsaturated infiltration and redistribution above the saturated zone.

3.4 Saint-Venant equations

The Saint-Venant equations, first developed by Barre de Saint-Venant in 1871, describe one-dimensional unsteady open channel flow. The Saint-Venant equations have various simplified forms, each defining a one-dimensional distributed routing model. The simplest distributed model is the kinematic wave model, which neglect the local acceleration, convective acceleration and pressure terms in the momentum equation; that is, it assumes $S_0 = S_f$ and the friction and gravity forces balance each other. The diffusion wave model neglects the local and convective acceleration terms but incorporates the pressure term. And finally the dynamic wave model considers all the acceleration and pressure terms in the momentum equation. An overview is given in the next table:

Table 3a. Summary of the Saint-Venant equations[1]

Continuity equation

Conservation form $\quad \frac{\partial Q}{\partial x} + \frac{\partial A}{\partial t} = 0$

Non conservation form $\quad V\frac{\partial y}{\partial x} + y\frac{\partial V}{\partial x} + \frac{\partial y}{\partial t} = 0$

Momentum equation

Conservation form

$$\frac{1}{A}\frac{\partial Q}{\partial t} + \frac{1}{A}\frac{\partial}{\partial x}\left(\frac{Q^2}{A}\right) + g\frac{\partial y}{\partial x} - g(S_0 - S_f) = 0$$

Local acceleration term	Convective acceleration term	Pressure force term	Gravity force term	Friction force term

[1]Neglecting lateral inflow, wind shear, and eddy losses, and assuming $\beta = 1$.

Non conservation form (unit width element)

$$(3.16)\quad \frac{\partial V}{\partial t} + V\frac{\partial V}{\partial x} + g\frac{\partial y}{\partial x} - g(S_0 - S_f) = 0$$

|----------Kinematic wave
|----------Diffusion wave
|----------Dynamic wave

3.5 The hillslope as a whole

Where the primary interest is in forecasting flows from whole catchments of more than 1 km^2, then both the cost of providing very detailed data and the computation involved argue for a highly simplified view of the hillslope. This means a highly simplified description of the physical processes mentioned above in a catchment. The model under study, the TOPMODEL, can be considered as such a model. The next chapter will give a presentation of the TOPMODEL and an explanation of the assumptions made of the physical processes described above.

4. DESCRIPTION OF THE TOPMODEL

4.1 Introduction

TOPMODEL (Beven and Kirkby, 1979; Sivapalan et al., 1987) introduces the use of topography in hydrological modelling. This runoff generating model relies on a topographic index to predict saturation excess runoff and on Philip's infiltration equation to predict infiltration excess runoff. "TOPMODEL is a variable contributing area conceptual model in which the predominant factors determining the formation of runoff are represented by the topography of the basin and a negative exponential law linking the transmissivity of the soil with the distance of the saturated zone below ground level" (Franchini et al, 1993). Although synthetic, this model is described by Sivapalan et al. (1987) as a "simple physically based conceptual model" in the sense that its parameters can be measured directly in situ. This definition is somewhat optimistic in view of the considerable simplification inherent in the structure of the model and the doubts and uncertainties encountered in defining the parameters of "physical models" themselves. But the inclusion of the effects of variability in rainfalls, soil characteristics, and topography on contributing area dynamics represents a major advance over previous models based on "point" hydrological response models assumed to apply at the catchment scale. Many simplifying assumptions have been made regarding the hydrologic processes taking place at the catchment scale. For example rainfall has been assumed to be constant in time during the storm event while being spatial variable; downslope redistribution of moisture during the storm has been neglected; and spatial correlation's in soils and rainfall are ignored. Also, the effects of micro topography on infiltration rates are neglected. Sivapalan et al. (1987), state that although these assumptions have been necessary to keep the model simple, it is expected that in time, many of these can be relaxed while retaining the concept of similarity between disparate catchments.

Two components can be identified in all conceptual rainfall-runoff models: the first represents the water balance at soil level and the second the transfer to the basin outlet. In the TOPMODEL, by its very nature, the flow in the soil is available directly along the drainage network, while the surface runoff component is made available to the drainage network inside each time interval: the saturated areas have, a limited extension around the drainage network.

The next paragraphs will concentrate mainly on a description of what represents the water balance component at the soil level and actually characterises the TOPMODEL. In this the following components are identified: canopy interception capacity, surface runoff due to saturation excess, surface runoff due to infiltration excess and, the flow in the saturated zone, the initial conditions and the computational procedure for the topographic index, and finally a paragraph where the whole model is revised.

4.2 Canopy interception capacity

What is described here as the canopy interception capacity and indicated by the symbol SR_{max} is described in many other articles as "Soil Root capacity" (c.f. for example Durand et al, 1992). In fact this component is not involved in the exchanges between unsaturated and saturated zones and its sole purpose is that of accumulation from which the water is extracted by potential rate evapotranspiration. It's very "starting position" in the chain of calculations inside the "program" basically assigns to it the role of intercepting available precipitation. This is why in this chapter, conform the paper of Franchini et al. (1993), it is preferred to present this component with the name "canopy interception capacity" rather than "soil root capacity".

The canopy interception capacity is represented by a reservoir with a capacity of SR_{max}. The water is extracted from the reservoir on the basis of the rate of potential evapotranspiration; the net precipitation (represented by the difference between precipitation and evapotranspiration) in excess of the capacity SR_{max} reaches the soil and comprises the input for the subsequent model components.

4.3 Surface runoff due to saturation excess

Appendix 6 describes a schematic representation of a valley and the formation of runoff according to TOPMODEL. The knowledge of initial conditions like the initial water table profile and the soil moisture profile in the unsaturated zone above the water table are mostly not available. Therefore it will be assumed that a reasonable approximation of the initial condition can be obtained by assuming that the recession discharge prior to a storm period $Q(0)$ results from a steady rate of recharge to the water table.
In TOPMODEL it is assumed that the saturated hydraulic conductivity within the soil profile follows an exponential decay with depth of the form:

(4.1) $$K_s(z) = K_0 \exp(-fz)$$

K_s = the saturated hydraulic conductivity;
z = depth in the soil (see footnote [2])

[2] The variable $z \equiv z_i$ represents the depth of the "water-table" in relation to the surface of the soil. In other articles (e.g. Beven et al., 1988) the reference variable is represented by the "moisture deficit" S_i, which is nevertheless linked to the variable z_i through the equation $S_i = (\theta_s - \theta_r) z_i$, where θ_s and θ_r represent, respectively, the moisture content in the saturated soil and the residual moisture content. The equations characterising the model written in terms of S_i are entirely identical to the preceding ones (cf. Beven et al. 1988) except that z_i is replaced by $z_i = S_i / (\theta_s - \theta_r) = S_i / \Delta\theta$, or z_i is substituted with S_i and the parameter $m = \Delta\theta / f$ is introduced. Below, unless specified otherwise, reference will nevertheless be made to the equations written directly in terms of depth z_i and transmissivity $T_0 = K_0 / f$

K_0 = hydraulic conductivity at ground level. Which in the version of Franchini et al. (1993) is held to be constant over the entire basin

f = decay factor of K_s with z. Held to be constant over the entire basin.

The "water table" (c.f. Sivapalan et al, 1987) is taken to be parallel to the ground surface (appendix 6), so that downslope flow beneath a water table at a depth z_i is given for any point i by:

(4.2) $$q_i = T_i(z_i)\tan\beta_i$$

$\tan\beta_i$ = surface slope of soil at point i

$T_i(z_i)$ = transmissivity at point i

The value of $T_i(z_i)$ is a transmissivity that varies non linearly with depth to the water table and is given by integrating equation (4.1) from the bottom of the profile at depth Z to the water table depth as:

(4.3) $$T_i(z_i) = \int_{z_i}^{Z} K_s(z)dz = \frac{K_0}{f}\left[\exp(-fz_i) - \exp(-fZ)\right]$$

$$= \frac{1}{f}\left[K_s(z_i) - K_s(Z)\right]$$

Equation (4.3) assumes that downslope flows within the capillary fringe are negligible, even though the soil is nearly saturated. In TOPMODEL this is justified on the consideration that near surface saturated conductivity's are dominated by flow through the small volume of structural voids and macro porosity of the soil that will be drained in the capillary fringe in equation (4.3). For large f or Z, exp (-fZ) can be assumed small. Substituting in equation (4.2) yields:

(4.4) $$q_i = \frac{K_0}{f}\tan\beta_i \exp(-fz_i)$$

$$= T_0 \tan\beta_i \exp(-fz_i)$$

where $T_0 = K_0 / f$ is the transmissivity coefficient of the whole profile, which is, like K_0 and f, constant over the whole basin.

For a quasi steady state condition with a spatially uniform recharge rate R to the water table is considered:

(4.5) $$a_i R = T_0 \tan\beta_i \exp(-fz_i)$$

where:

R = uniform recharge rate to the water table.

a_i = area draining through location i, per unit contour length.

Making z_i explicit in equation (4.5) gives:

$$(4.6) \quad z_i = -\frac{1}{f}\ln\left(\frac{a_i R}{T_0 \tan\beta_i}\right)$$

By integrating over the entire area of the basin and dividing by the entire area, the mean value is obtained of the variable z_i:

$$(4.7) \quad \bar{z} = \frac{1}{A}\int_A z_i dA$$

$$= \frac{1}{fA}\int_A \left[-\ln\left(\frac{a_i}{T_0 \tan\beta_i}\right) - \ln R\right] dA$$

where A is the entire area of the basin. It is allowed that the equation (4.2) continues to hold for water tables rising above the soil surface, i.e. for negative values of z_i.
Using eq.(4.5) to substitute for R in eq.(4.7), gives:

$$\bar{z} = \frac{1}{f}\left[-\frac{1}{A}\int_A \ln\left(\frac{a_i}{T_0 \tan\beta_i}\right) dA + fz_i + \ln\left(\frac{a_i}{T_0 \tan\beta_i}\right)\right]$$

or:

$$(4.8) \quad f\cdot(\bar{z} - z_i) = \left[\ln\frac{a_i}{\tan\beta_i} - \lambda\right] - \left[\ln T_0 - \ln T_e\right]$$

where: $$\lambda = \frac{1}{A}\int_A \ln\frac{a_i}{\tan\beta_i} dA$$

and: $$\ln T_e = \frac{1}{A}\int_A \ln T_0 \, dA$$

Equation (4.8) expresses, in dimension-less form, the deviation of the local depth of the water table, scaled by the parameter f, in terms of the deviation in the logarithm of transmissivity away from the areal integral value $\ln T_e$, and a deviation in the local topographic index away from its areal integral value λ, the catchment topographic constant of Beven en Kirkby (1979).
Values of these deviations that yield z_i less than or equal to the depth of the capillary fringe ψ_c for a given value of $\bar{z}$ are of particular interest in that they represent the predicted area of saturated soil, which will act as a saturation excess contributing area.
Equation (4.8), the local depth to the water table z_i, may also be expressed in the form:

$$(4.9) \quad z_i = \bar{z} - \frac{1}{f}\left[\ln\left(\frac{a_i T_e}{T_0 \tan\beta_i}\right) - \lambda\right]$$

were $\ln(a_i T_e / T_0 \tan\beta_i)$ is a combined topography-soil index and $\ln(T_e)$ is the expected value of $\ln(T_0)$. λ is the expected value of the topographic index $\ln(a / \tan\beta)$.
According to the latest application of TOPMODEL (Franchini et al., 1993), it is stated that in the case of constant transmissivity we can write:

$$(4.10) \quad \lambda = \frac{1}{A}\int_A \ln\frac{a_i}{T_0 \tan\beta_i} dA$$

$$= E\left[\ln\frac{a_i}{T_0 \tan\beta_i}\right]$$

$$= E\left[\ln\frac{a_i}{\tan\beta_i}\right] - \ln T_0$$

where E stands for Expected value,
and therefore:

$$(4.11) \text{ (a)} \quad \lambda = \lambda^* - \ln T_0 \qquad \text{(b)} \quad \lambda^* = E\left[\ln\frac{a_i}{\tan\beta_i}\right]$$

Thus, equation (4.9) becomes:

$$(4.12) \quad z_i = \bar{z} - \frac{1}{f}\left[\ln\frac{a_i}{\tan\beta_i} - (\lambda + \ln T_0)\right]$$

$$z_i = \bar{z} - \frac{1}{f}\left[\ln\frac{a_i}{\tan\beta_i} - \lambda^*\right]$$

In other words the calculation of the depth z_i of the "groundwater" is determined only by the parameter f and the topographic index $x = \ln\frac{a}{\tan\beta}$.
Franchini et al. (1993) presumed that the transmissivity (linked with the hydraulic conductivity (K_0) by $T_0 = K_0 / f$), is constant over the whole basin and use instead of eq. (4.9) from Sivapalan et al. 1987 the latest called equation (4.12).

This means that the don't use the so called "combined topography-soil index" and the expected value of $\ln(T_e)$ or $\ln(T_0)$, but only the topographic index to determine the saturated part of the soil.

If $z_i \leq 0$ then the "water-table" is, at least, at level with the surface of the soil and therefore at this point *-i-* the saturation condition has been reached. All the points with $z_i \leq 0$ generate the basin fraction in saturation conditions where the rainfall produces direct surface runoff. Equation (4.12) shows that it is not the actual position of the *i*-th point which is important, but the value of the topographic index $x = \ln \frac{a}{\tan\beta}$; moreover, from equation (4.12) if x^* is the value of x which produces $z_i = 0$, then all the points with $x \geq x^*$ are in saturation conditions. The basin percentage with $x \geq x^*$ is then defined on the basis of the index curve which in turn represents the probability distribution of the variable x. The method used of computing this variable, based on a Digital Terrain Map (DTM) and the index curve which are described in paragraph 4.7.

4.4 Calculation of runoff from infiltration excess

The surface runoff due to infiltration excess is the component described in Sivapalan et al. (1987) and in Wood et al. (1988) is based on the Philip scheme (1957):

(4.13) $g = cK_0 + \frac{1}{2} St^{-1/2}$

where g is the infiltration capacity, S the "sorptivity", and K_0 the saturated hydraulic conductivity at the soil level. The "sorptivity" S is linked with K_0 as follows:

(4.14) $S = S_r K_0^{1/2}$

In the version of Sivapalan et al. (1987), K_0 may be considered randomly variable over the whole basin while S_r and c are regarded as constant. They assume that the infiltration capacity at the soil surface is controlled by the initial surface moisture content and the saturated hydraulic conductivity of the surface layer. They neglect the variation of these quantities with depth. Which in turn allows an analytical solution for the infiltration process for the case of spatially variable rainfalls and soil characteristics. The infiltration rate due to a rainfall of intensity p has been derived by Sivapalan and Wood (1986). An infiltration model which does take the decline of conductivity with depth into account is available (Beven, 1984, 1986a,b), but is less analytically tractable.

In the most recent study of Franchini et al. (1993), K_0 is considered constant. The K_0 obtained during calibration in that report are so high (because the use of great grid sizes) that no type of Hortonian mechanism has ever been activated.

This means that TOPMODEL in practical applications denies the possibility of representing the surface runoff formation process from infiltration excess, since the rainfall intensity will never acquire values comparable with that of the parameter K_0. For the more specific equations of infiltration excess used in TOPMODEL will therefore be referred to the article of Sivapalan et al. (1987).

4.5 Calculation of the flow in the saturated zone and sequence of calculations in the TOPMODEL

Equation (4.12) permits the estimation of the saturated basin fraction on the basis of the knowledge of the current value of $\bar{z}$. The value of $\bar{z}$ is updated at every Δt on the basis of the following equation:

$$(4.15)\quad \bar{z}^{t+1} = \bar{z}^{t} - \frac{\left(Q_V^t - Q_B^t\right)}{A}\Delta t \qquad \text{(continuity equation)}$$

where:

Q_V^t	=	Recharge rate of the saturated zone from the unsaturated zone over the time interval $t/(t+\Delta t)$;
Q_B^t	=	"Base flow", connected to the flow in the saturated zone, over the time interval $t/(t+\Delta t)$;
A	=	Area of the basin;
Δt	=	Time interval.

The quantity Q_B^t can be defined analytically:

$$(4.16)\quad Q_B^t = \int_L Q_{B_i}^t \, dL$$

$$= \int_L T_0 \tan\beta \exp\left[-f\, z_i^t\right] dL$$

where L is twice the length of all channels contributing to base flow. Bearing in mind equation (4.12), we can write:

$$Q_B^t = \int_L T_0 \tan\beta \exp\left[-f\,\bar{z}^t - \lambda^* + \ln\frac{a}{\tan\beta}\right]$$

$$= T_0 \exp\left[-f\,\bar{z}^t\right] \cdot \exp\left[-\lambda^*\right] \cdot \int_L a \cdot dL$$

Since:

$\int_L a \cdot dL = A$ (total area of basin)

we get:

(4.17) $Q_B^t = A \cdot T_0 \cdot \exp[-\lambda^*] \cdot \exp[-f\,\bar{z}^t]$

$= Q_0 \cdot \exp[-f\,\bar{z}^t]$

with: $Q_0 = A \cdot T_0 \cdot \exp[-\lambda^*]$

Q_V^t is calculated as the sum of the contribution of all the grids covering the basin:

(4.18) $Q_V^t = \sum_{i \in A} Q_{V_i}^t = \sum_{i \in A} \alpha_i K_0 \exp[-f\,z_i^t]$

where α_i is the area of the i-th grid. Naturally equation (4.18) holds good when the current moisture content in the unsaturated zone is not a limiting factor; otherwise the contribution is calculated on the basis of the actual amount of water available. Equation (4.18) extends to all the grids where $z_i \geq 0$.

4.6 Initial conditions

4.6.1 Prior to storm rainfall

The continuity equation (4.15) is initialised assuming that the simulation begins after a long dry period; in other words the unsaturated zone in TOPMODEL is held to be totally dry and the flow observed at the basin outlet is considered to have been generated only by the "base contribution":

$$Q_V^1 = 0$$
$$Q_B^1 = Q_{ob}^1$$

Recalling equation (4.17), we get:

$$Q_B^1 = Q_0 \exp(-f \cdot \bar{z}^1)$$

and therefore:

(4.19) $\bar{z}^1 = -\frac{1}{f} \ln\left(\frac{Q_{ob}^1}{Q_0}\right)$

With equation (4.12) it is possible to define the initial depth of the "groundwater" in each grid.

4.6.2 In the unsaturated zone

During a storm the production of runoff will depend on the unsaturated zone moisture profile. Infiltration excess runoff will depend primarily on the local surface hydraulic conductivity and initial surface moisture content. Production of saturation excess runoff will depend on the local moisture storage deficit at any point. For simplicity, downslope redistribution of moisture within the duration of the storm is neglected in TOPMODEL. It is assumed that saturated excess runoff will be generated wherever the cumulative infiltration volume exceeds the initial soil moisture storage deficit. This may be predicted from the depth to the water table by assuming that the unsaturated zone profile is close to the case of complete gravity drainage. For this the soil moisture characteristic relationships of Brooks and Corey (1964), are used:

$$K(\psi) = K_s \left(\frac{\psi_c}{\psi} \right)^{2+3B} \qquad \text{with: } \psi \le \psi_c$$

$$K(\psi) = K_s \qquad \text{with: } \psi \ge \psi_c$$

$$\theta\ (\psi) = \theta_r + (\theta_s - \theta_r) \left(\frac{\psi_c}{\psi} \right)^{B} \qquad \text{with: } \psi \le \psi_c$$

$$\theta\ (\psi) = \theta_s \qquad \text{with: } \psi \ge \psi_c$$

where ψ_c is the depth of the capillary fringe, ψ is the matrix head equal to z_i - z, θ_s is the saturated moisture content, and θ_r is the residual moisture content and B is a pore size distribution index (c.f. Troch et al., 1993a). In the article of Sivapalan et al. 1987, is assumed that the saturated moisture content is constant with depth. The total profile moisture deficit (S_i) may then be obtained by integrating from the surface to the top of the capillary fringe as:

$$(4.20)\quad S_i = (\theta_s - \theta_r) \left[z_i - \psi_c - \frac{1}{1-B} \left[\left(\frac{\psi_c}{z_i} \right)^{B} z_i - \psi_c \right] \right]$$

4.7 Description of the computational procedure for $x = \ln \frac{a}{\tan\beta}$ in each grid

The TOPMODEL involves the use of Digital Terrain Maps (DTM) to determine an index representing the potentiality of the soil to become saturated with water. The DTM is a topographical configuration of an area with a matrix representing the altitude of a region at a given grid size.
Equation (4.12) shows that the real position of the pixel i is of no interest, only the local value of $\ln \frac{a_i}{\tan\beta_i}$ is important. Thus all the information represented in the two dimensional distribution of the index over a catchment can be concentrated in the one dimensional curve of the probability to have a given value of the index. This curve should be representative of the catchment on which it was build. Franchini et al. (1993) report however that the shape of these index curve's are not significantly different for different catchments. Now we are able to represent all the information in the two dimensional distribution of the index in a one dimensional curve of the density of probability to have a given value of the index as shown in figure 4a. But the curve really used by the TOPMODEL is the complementary to one of the cumulated probability, so that the percentage of saturated area knowing the minimum value of the index leading to saturation is directly visible as in figure 4b.

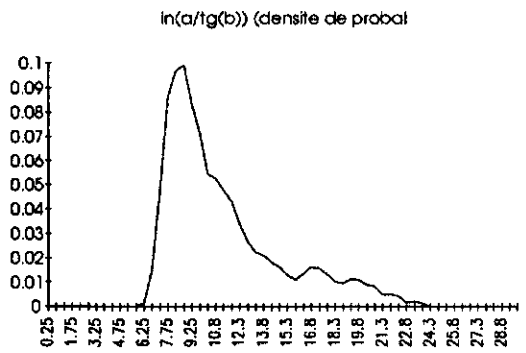

Figure 4a. Density of probability of $\ln(a/\tan\beta)$

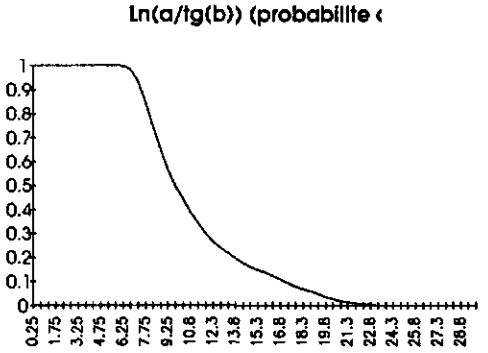

Figure 4b. Cumulative probability of $\ln(a/\tan\beta)$

In order to calculate $x = \ln \frac{a}{\tan\beta}$ in each grid we must calculate the contributing area for that grid and then divide by the tangent of the slope relevant to that grid. Only the downward directions are considered below. If we assume that all the directions have the same water transportation probability, then the area drained by contour unit of length can be calculated as (Quinn et al., 1991):

$$(4.21) \quad a = \frac{A}{nL}$$

where:

n = number of downstream directions;

L = effective contour length orthogonal to the direction of flow ($L = \frac{GS}{1+\sqrt{2}}$, with GS, Grid Size of the DTM (Digital Terrain Map));

A = total area drained by current grid (total upslope area).

One possible representation of tan(β) is:

$$(4.22)\quad \overline{\tan(\beta)} = \frac{1}{n}\sum_{i=1}^{n}\tan(\beta_i)$$

where $\tan(\beta_i)$ is the slope of the line connecting the current grid with the furthermost grid in the i-th downstream direction. Therefore:

$$(4.23)\quad \frac{a}{\overline{\tan(\beta)}} = \frac{A}{L\sum_{i=1}^{n}\tan(\beta_i)} \qquad \text{and} \qquad \ln\left(\frac{a}{\overline{\tan(\beta)}}\right) = \ln\left(\frac{A}{L\sum_{i=1}^{n}\tan(\beta_i)}\right)$$

The amount of A that contributes in each downstream direction i is thus calculated as:

$$(4.24)\quad \Delta A_i = \frac{A\cdot\tan(\beta_i)}{\sum_{i=1}^{n}\tan(\beta_i)}$$

The procedure is repeated on all the DTM grids proceeding downstream. The function regarding the exceeding of $x = \ln(a/\tan\beta)$, i.e. the basin's index curve, together with the equation (4.12), enables to define both the percentage of the basin in saturated conditions and the shape of the water table which marks off the upper limit of the saturated zone in the soil. Of all the factors affecting the formation of runoff, the index curve (see figure 4b) represents the "topography" component or rather the "slopes" which, in this model, constitute the driving force for the interflow.

4.8 Revision of the TOPMODEL

The rainfall-runoff transformation process in the best known models is based on an equation or "sub-model" identifying the physical factors affecting the formation of runoff. When this input doesn't consider the spatial variability, it is mostly presented by a probability function, that is ignoring the real distribution (Moore and Clarke, 1981; Moore, 1985).

By contrast to what happens in other rainfall-runoff models, the probability law for the TOPMODEL is defined on the basis of the topography of the basin (the index curve, see figure 4b) and it's input into the model by using DTM. The index curve however is greatly affected by the size of the DTM grid and this dependence is reflected in the parameter K_0.

Franchini et al. (1993) report that the TOPMODEL is surprisingly insensitive to the basin's actual index curve. Therefore it is possible to do without the calibration process for this index curve. This leads to the great advantage of the TOPMODEL with other rainfall-runoff models. Franchini and Pacciani (1991) pointed out that the difficulty of using rainfall-runoff models in general is the increasing number of parameters to be estimated. The only parameters that need to be calibrated in TOPMODEL are f and K_0 (or, the transmissivity T_0, which is however linked to the previous two by the equation $T_0 = K_0 / f$, representing the nature of the soil) and the parameter SR_{max} representing the leaf capacity. The parameter K_0 is introduced into the TOPMODEL by means of the Darcy law relating to interflow. It must however be interpreted as an artificial hydraulic conductivity that incorporates both the actual hydraulic characteristic of the soil and the spatial expansion effect connected with the size of the grid.

Franchini et al. (1993) also expressed that as a result of the systematic increase in K_0 with the size of the DTM grid, the TOPMODEL in practical applications, denies the possibility of representing the surface runoff formation process from infiltration excess, since no Hortanian process will take place. In fact all the runoff will occur in saturated conditions. The relative proximity of the saturated zone to the surface of the soil caused by equation (4.1), combined with the high hydraulic conductivity value, are such that at each time step the unsaturated zone accumulates all the precipitation and at the same time yields it to the saturated zone, thus remaining systematically dry. The next chapter will give some considerations about these last mentioned points and discusses the possible ways of improving these imperfections.

5. DESCRIPTION OF THE PROBLEMS IN TOPMODEL AND THE ALTERNATIVE SOLUTIONS

The TOPMODEL is recently used for many catchment descriptions, where it gives reasonable till good results (Wood et al., 1988; Durand et al., 1992; Troch et al, 1993a,b; Franchini et al. 1993). To check of this is true, a single run of the TOPMODEL has been performed and is reported in the paragraph below.

5.1 A small experiment with TOPMODEL

Although it is not within the scope of this report to do a calibration of the TOPMODEL, a single run has been performed. For this experiment data of the Reno river catchment in Italy has been used. The Reno river flows north from the Apennine mountains before reaching the Po valley were it bends to the east to join eventually the Adriatic sea (see appendix 7). The Reno basin itself is about 210 km long and drains 4000 km^2 at the sea. The mountain part has altitudes up to 2000 meters and the Reno valley is surrounded by quite steeply slopes in its highest part. It is in these mountainous and most natural part of the catchment that the a sub-catchment of about 1000 km^2 is selected (see appendix 7).
Appendix 8 shows the results of the calibration for the data over the period of February 1990 till May 1990. And appendix 9 shows the validation of the TOPMODEL with data of the rest of the year 1990. The uninterrupted line is the observed discharge, the dashed-dotted line is the calculated discharge and the dotted line is the base flow.
It should hereby be mentioned that the selected sub-catchment contains three hydroelectric power plants, controlling more or less a quarter of the total sub-catchment. These three reservoirs, even if not very big compared to the average volume available on these sort of hydraulic works (10 million m^3 as a total), are nevertheless able to cut down the flood wave or at the contrary to increase the recession flows. The output discharges of these reservoirs however were not available and therefore not taken into account by running the TOPMODEL. In spite of this infirmity the results of forecasting are quite good.
Table 1 shows the explained variance, the determination coefficient and the correlation coefficient of both the calibration as well as the validation periods. These mathematical definitions all have a maximum of 1, and as we can see the results are quite reasonable reaching from 0.7 till 0.93. However looking at Table 2 we can see that there are some unrealistic values for the parameters that have a physical meaning such as the hydraulic conductivity and the exponential decay rate of transmissivity with depth. The next two paragraphs will discuss these problems in depth and the last paragraph of this chapter will reach some alternative solutions, which will be worked out in the next chapter.

5.2 The case of artificial high hydraulic conductivity

First of all there is the variation of the hydraulic conductivity factor (K_0) in relation with the grid size of the DTM. As stated in the previous chapter the value of K_0 increases to artificial values if the size of the grid increases. This problem could arises from the fact that TOPMODEL considers a grid-cell in a quasi steady state condition.
The physical analysis of a hydraulic system is usually addressed using the momentum equation and the continuity equation. In the TOPMODEL the momentum equation is represented by a derivation of the Darcy equation, in the form (see paragraph 4.3):

(4.4) $q_i = T_0 \tan\beta_i \exp(-fz_i)$

The continuity equation, expressed in integrated form in space, generally takes the form:

(5.1) $\frac{dS}{dt} = I - O$

where I and O represent two time functions of the incoming and outgoing quantity respectively, while S represents the storage of the "system" and t is the time.
In the TOPMODEL the system to which the continuity equation refers is represented by the saturated zone; in it the input function is the net precipitation while the output function is the flow in the saturated zone. The steady state assumption entails writing the continuity equation as in equation (4.5, paragraph 4.3):

(4.5) $a_i R = T_0 \tan\beta_i \exp(-fz_i)$

This implies that $\frac{dS}{dt} = 0$ in each grid cell, i.e. in the saturated zone there is no time delay in routing water between the upstream point and downstream point of the grid cell. But with the increasing of the grid-cell this hypotheses tends to loose its value. In TOPMODEL water is supposed to be transported within one time step. Looking at equation (4.5), we can see that if a is increasing, because of the increasing grid size (see relation with grid size in equation (4.21)), the transmissivity T_0 (with is related with K_0 by $T_0 = K_0 / f$) has to increase, to keep the equation in balance. Thus increasing grid size leads to increasing K_0 values. Franchini et al. (1993) reported values of K_0 = 35 m/h and f = 58.8 m^{-1} with a grid size of 60 x 60 m. ($T_0 \approx 0.6\ m^2h^{-1}$) up till K_0 = 300 m/h and f = 66.67 m^{-1} with a grid size of 400 x 400 m. ($T_0 \approx 4.5\ m^2h^{-1}$).
They also calculated for a certain catchment, by interpolating DTM in the continuum (this means a grid size of zero), a K_0 of 0.57 m/h. This value is certainly closer to reality but has no use in the application of TOPMODEL.

Durand et al. (1992) also report a high maximum transmissivity reaching from 11.6 m^2h^{-1} till 14.8 m^2h^{-1}, with the use of a grid size of 25 x 25 m. Astounding however is that they don't consider these values as unrealistic, as they state:

> "These values do not seem unrealistic, owing to the very coarse texture of the soils (50-60% coarse sand) and the abundance of blocks and outcrops"

A possible solution to the problem described above could be to get rid of the steady state hypotheses in a grid-cell. In that case we can establish a correct continuity equation which doesn't suggest a stationary condition at grid dimension.
Instead of assuming transport within a grid-cell in one time step we can use the kinematic wave as a more correct way for rooting approximation. This should allow a K_0 value more close to the physically real one and maintains the simplicity of the model. This because we don't need to route all the water immediately from the upstream boundary to the downstream one of the grid cell.

5.3 Hydraulic conductivity related with moisture content

The second problem is the discussed form of the saturated conductivity coefficient. In the TOPMODEL K_s has been assumed to by a negative exponential function of depth as follows in equation (4.1, see paragraph 4.3):

(4.1) $$K_s(z) = K_0 \exp(-fz)$$

Using values for K_0 and f obtained from the report of Franchini et al. (1993), we get graphs of this equation as shown in figure 5a and 5b.

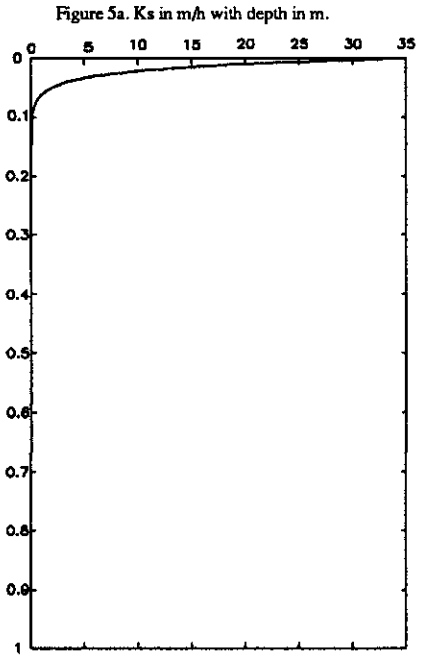

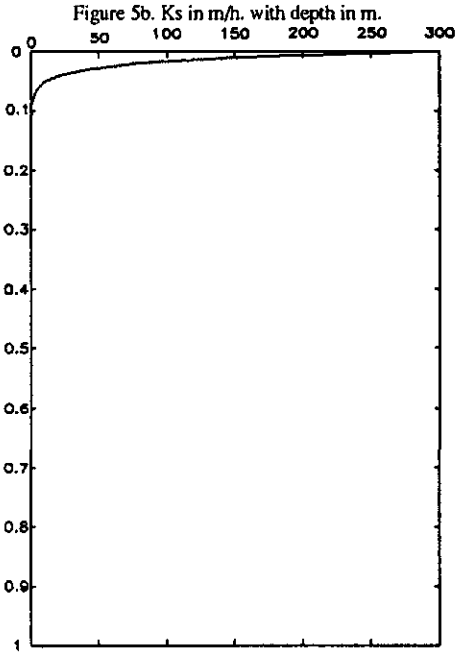

Figure 5a shows equation (4.1) for the values of K_s, when K_0 = 35 m/h. and f = 58.8 m^{-1} and **figure 5b** shows equation (4.1) for the values of K_s when K_0 = 300 m/h. and f = 66.67 m^{-1}. Values are obtained from Franchini et al., 1993.

Looking at figures 5a and 5b it has to be considered that z is the first meter of *water* in the soil (i.e. without the soil component). As we can see from figure 5a,b, the TOPMODEL application made by Franchini et al., 1993, considers a unrealistic high saturated hydraulic conductivity found in the first few centimetres under the soil surface. A similar behaviour can be obtained also from the values used by Durand et al. (1992). Since flow in the subsurface in TOPMODEL only occurs in saturated conditions, this will take place in these few centimetres under the soil surface.

This formulation gives rise to some discussion. TOPMODEL neglect flow that occurs in the unsaturated zone. However looking at reality we see that macropores and other structural channels in the rootzone (Beven and Germann, 1982) not only give rise to a high hydraulic conductivity but also to a lateral flow in the unsaturated zone on a hillslope. Many other authors stated that flow in the unsaturated zone of a catchment is of significant importance (Freeze, 1972b; Sloan and Moore, 1984; Stagnitti et al., 1986).

To take the process of flow through the unsaturated zone into account we introduce the dependence of hydraulic conductivity with moisture content. TOPMODEL doesn't consider this as we can see in equation (4.4), where flow is calculated only from transmissivity in saturated conditions. The next paragraph will discuss different ways of describing hydraulic conductivity with moisture content and will introduce a new analytical description for this process.

5.4 Alternative solutions

Description of horizontal flow in unsaturated conditions could be made basing upon the knowledge of the vertical moisture content profile into the soil. Due to the high conductivity value, caused by macropores in the top of the soil (Beven and Germann, 1982), gravity will be the dominant mechanism driving water from the top of the soil to the bottom (impermeable or semi impermeable lower boundary). The latter mentioned boundary will create a perched water table. In this zone a not negligible horizontal propagation (also involving unsaturated flow), will occur.

Nevertheless, the depth of this high conductive soil will be negligible with respect to the horizontal grid dimensions. This allows the transient phase of vertical propagation to be neglected. We will take into account a succession of equilibrium profiles in the vertical. A further simplification can be introduced making reference to the integral value of the vertical moisture content, instead of the real vertical equilibrium profile, in the view of the hillslope propagation. It will be examined if horizontal flow (or hydraulic conductivity) evaluated starting from a real vertical equilibrium profile and that deriving from the integral moisture content are comparable.

Therefore we calculate hydraulic conductivity from a number of different vertical profiles. These profiles have a variation of moisture content with depth with the same total moisture content ($\bar{\theta}$). A number of different $\bar{\theta}$ values have been taken into account, ranging from 0 to 1. The purpose is to compare this conductivity value with that coming from the consideration of the integral moisture content with no reference to the real vertical profile.

5.4.1 Relations of hydraulic conductivity with moisture content

Two different relationships that both describe hydraulic conductivity with moisture content in a different way are found in the literature and compared with the analytical description we developed for describing this process, as will be introduced later.

First of all there is the relationship derived from Brooks and Corey (1964) relating hydraulic conductivity and moisture content (θ). The formulation is derived from the relationships as mentioned in paragraph 4.6.2. The transformation is as follows:

from $\theta\ (\psi) = \theta_r + (\theta_s - \theta_r)\left(\frac{\psi_c}{\psi}\right)^B$

we can write $\frac{\psi_c}{\psi} = \left[\frac{\theta - \theta_r}{\theta_s - \theta_r}\right]^{1/B}$

which substituted in $K(\psi) = K_s \left(\frac{\psi_c}{\psi} \right)^{2+3B}$ gives $K(\psi) = K_s \left[\frac{\theta - \theta_r}{\theta_s - \theta_r} \right]^{\frac{2+3B}{B}}$ which can be rewritten as the next equation:

(5.2) $K(\theta) = K_s \ \bar{\theta}^c$

where: $K(\theta)$ = hydraulic conductivity as a function of moisture content

K_s = saturated hydraulic conductivity

$\bar{\theta}$ = reduced moisture content $(\theta - \theta_r)/(\theta_s - \theta_r)$, reaching from 0 till 1

c = a pore size distribution factor (first expressed in B), which will be a constant

This equations leads to a graph as shown in appendix 10. Brooks and Corey (1964) obtained fairly accurate predictions with their equations.

The second relationship that will be compared with ours is the one of van Genuchten (1980). He describes in his paper a relatively simple equation for the soil-moisture content-pressure head curve, $\theta(h)$. The resulting expressions for $K_r(\bar{\theta})$ contain three independent parameters which may be obtained by fitting the proposed soil-water retention model to experimental data. An attractive class of $\bar{\theta}(h)$-functions, adopted in van Genuchten's study is given by the following general equation:

(5.3) $\bar{\theta} = \left[\frac{1}{1 + (\alpha h)^n} \right]^m$

where: $\bar{\theta}$ = reduced moisture content $(\theta - \theta_r)/(\theta_s - \theta_r)$, reaching from 0 till 1

h = the pressure head

and α, n, m = parameters

Van Genuchten derived his equations from two different points of departure. The first one leads to a relative hydraulic conductivity related to moisture content as:

(5.4) $K_r(\bar{\theta}) = \bar{\theta}^{1/2} \left[1 - \left(1 - \bar{\theta}^{1/m} \right)^m \right]^2$ with restrictions: $(m = 1 - 1/n)$ $(0 < m < 1)$

where: $K_r(\bar{\theta})$ = the relative hydraulic conductivity as a function of the dimensionless moisture content

m and n = parameters to be estimated

The second equation of van Genuchten (1980) leads to a hydraulic conductivity related to moisture content as:

$$(5.5)\quad K_r(\bar{\theta}) = \bar{\theta}^2\left[1-\left(1-\bar{\theta}^{1/m}\right)^m\right] \text{ with restrictions: } \begin{matrix}(m = 1-2/n)\\(0<m<1; n>2)\end{matrix}$$

where: $K_r(\bar{\theta})$ = the relative hydraulic conductivity as a function of the dimensionless moisture content

m and n = parameters to be estimated

Equations (5.4) and (5.5) can be rewritten to the hydraulic conductivity instead of the relatieve hydraulic conductivity. Equation (5.4) will then look like:

$$(5.6)\quad K(\bar{\theta}) = K_s.\bar{\theta}^{LL}.\left(1-\left(1-\bar{\theta}^{1/m}\right)^m\right)^2 \text{ with restrictions: } \begin{matrix}(m = 1-1/n)\\(0<m<1)\end{matrix}$$

where: $K(\bar{\theta})$ = the hydraulic conductivity related with the dimensionless moisture content

LL = a parameter to be estimated

The last mentioned equation (5.6) has the shape of our analytical description introduced in the next subparagraph. This analytical expression will be compared and fitted with equation (5.6), with the use of a technical computing environment for high-performance numeric computation and visualisation, called MATLAB, to show that they give more or less the same results.

5.4.2 An analytical derivation of hydraulic conductivity with moisture content

The description we developed and that is to be compared with that of Brooks and Corey and van Genuchten is, instead of the two above mentioned, an expression of hydraulic conductivity upon the *integral* moisture content. The fact that we are talking about the integral moisture content allows us to solve an analytical solution.

A full derivation of the analytical solution will be given in appendix 11. Only the final equations that follow from the derivations will be given below. First of all there is the moisture content (θ) dependence on depth (z). This equation shows eventually three parameters to be estimated to fit more or less the van Genuchten expressions:

$$(5.7)\quad \bar{\theta}_0^* = 1-(1-\bar{\theta}_0)\left(\frac{z^*}{L_1}\right)^{1/b} \qquad \text{N.B. } z^* \le L_T$$

where $\bar{\theta}_0^*$ = reduced moisture content at the surface of the profile

$\bar{\theta}_0$ = initial reduced moisture content, first parameter to be estimated

z^* = point starting from which you have saturation, could be the water-table but also the perched water-table

L_1 = artificial depth of the water table, second parameter to be estimated

b = third parameter to be estimated

L_T = depth of the impermeable or semi impermeable lower boundary, could be a parameter but is set in this study on 1 meter

Note that the L_1 value is not the real depth of the water table, but looking at equation (5.7) we have to divide by a length to have the dimensionless form on both sides of the equal sign. Figure 5c gives a systematisation of the process of the rising water-table as described in the equation above.

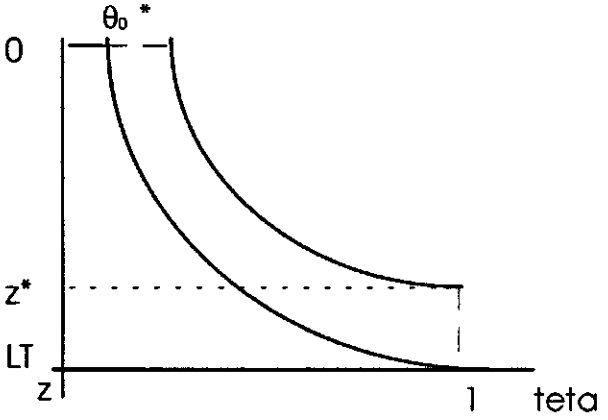

Figure 5c The process as mentioned in equation (5.7)

The second equation that is derived and must be fitted is the one that is describing the hydraulic conductivity (K) depending on reduced moisture content $(\bar{\theta})$. In this equation an extra parameter besides the three mentioned above most be estimated:

$$(5.8)\quad K(\bar{\theta}) = K_s\left[1-(1-\bar{\theta})^{1/c}\right] \qquad c>0$$

where $K(\bar{\theta})$ = hydraulic conductivity related to moisture content

K_s = saturated hydraulic conductivity

$\overline{\theta}$ = reduced moisture content $(\theta - \theta_r)/(\theta_s - \theta_r)$, reaching from 0 till 1

c = the extra parameter to be fitted

Now this equation (5.8) will be rewritten so that we will have an expression for the transmissivity in which only the value of the integral moisture content most be taken into account (see for derivation appendix 11):

$$(5.9) \quad T = K_s L_T \left[1 - \alpha \left(1 - \frac{\Theta}{L_T} \right)^{\beta} \right]$$

Where T = Transmissivity (measure for the ability of an aquifer to let water through, dimensions $[L^2T^{-1}]$)

$$\alpha = \left(\frac{L_1}{L_T} \right)^{\frac{c-1}{c(b+1)}} \frac{bc}{bc+1} (1-\theta_0)^{\frac{b(1-c)}{c(b+1)}} \left(\frac{b+1}{b} \right)^{\frac{bc+1}{c(b+1)}}$$

Θ = the integral water content over total depth z^*

$$\beta = \frac{bc+1}{c(b+1)}$$

The next chapter will give a further explanation of the solutions we had in mind for describing the process of horizontal flow in the unsaturated zone, and will give the results we obtained by doing so.

6. ELABORATED SOLUTIONS

As is described in chapter 4 and 5, flow routing in TOPMODEL in subsurface takes only place in saturated conditions. The unsaturated zone plays no role in routing or delay routing in subsurface flow. As stated by many authors (Beven, 1982; Sloan and Moore, 1984; Stagnitti et al., 1986) this is not conform with reality. An improvement in the estimation of the unsaturated soil propagation time pattern will therefore extend the physical bases of the model.

A simple water routing model needs to be used since the model complexity should not increase in a undesirable way. Therefore kinematic wave approximation has been selected. Moreover a kinematic wave approximation in subsurface flows (both in vertical as in horizontal direction) has been successfully tested by many authors (see Borah et al. 1980; Beven 1981, 1982, Charbeneau 1984; Sloan and Moore, 1984; Hurley and Pantelis, 1985; Stagnitti et al., 1986). This approximation will be described in the following paragraph.

6.1 Kinematic wave solution

Kinematic wave equations have been extensively used to model surface propagation. It is particularly useful for flood calculation. Kinematic hydrology is decidedly more hydraulically correct than some of the more common methods of flood estimation such as the rational method, time-area methods, the Soil Conservation Service (SCS) method and unit hydrograph methods. The kinematic method is based on the continuity equation and a flow resistance equation, both basic hydraulic equations.

It was the American hydrologist, Horton (generally associated with infiltration) who in 1933 carried out the earliest recorded scientific studies of overland flow. Later Keulegan (1945) applied the continuity and momentum equations conjunctively for overland flow analysis. He investigated the magnitude of the various terms in the dynamic equation of St. Venant and indicated that a simplified form of the equation, now termed the kinematic equation, would be adequate for overland flow (see paragraph 3.4).

Starting with the formulation of the kinematic wave theory by Lighthill and Whitham (1955), kinematic overland flow models have been utilised increasingly in hydrologic investigations. The first application of kinematic wave routing to overland flow and groundwater flow was by Henderson and Wooding (1964). The conditions under which the kinematic flow approximation holds for surface runoff were first investigated by Woolhiser and Liggett (1967); they found it is an accurate approximation to the full equations for most overland flow cases (cf. Stephenson et al., 1986).

In the last decade the use of kinematic wave equation for subsurface flow modelling increased in popularity. This kinematic wave approximation is based on a

simplification of the motion equation governing unsteady flows in the unsaturated medium. The underlying assumption is that energy gradients due to capillary forces are negligible in comparison with gravitational and frictional effects.

In a earlier study, Henderson and Wooding (1964), provide solutions for horizontal kinematic subsurface flow through a porous medium of constant permeability both for steady state and a rising water-table. They compare the extended Dupuit-Forchheimer equation to a further simplification of the flow equation in which it is assumed that the hydraulic gradient at any point within the saturated zone is equal to the bed slope. Beven (1981, 1982), gave in two papers about kinematic subsurface storm flow a kinematic wave equation valid in a sloping soil mantle of constant saturated hydraulic conductivity overlying a relative impermeable bedrock sloping surface. In the first article, mainly devoted to the study of horizontal propagation, Beven stated that this equation was a good approximation to the more correct extended Dupuit-Forchheimer equation (see Beven (1981) for further details). In the second article of Beven also the vertical propagation in the unsaturated zone was taken into account, to evaluate the time at which the wetting front reaches the bottom of the profile.

6.2 Model development

In a shallow soil layer overlaying an semi-impermeable bed the total amount of downslope flow can be derived by integrating in the vertical direction from surface to low permeable soil elevation the point based continuity equation.
A kinematic wave approximation of subsurface flow can be taken thus assuming flow lines in subsurface propagation to be parallel to the low permeable bottom layer and hydraulic gradients equal to the slope of this layer. The above mentioned hypotheses lead to the following partial differential equation:

$$(6.1) \quad L(\theta_s - \theta_r)\frac{\partial \overline{\Theta}}{\partial t} = -K_s \tan\beta \frac{\partial}{\partial y}\int_0^L \overline{\theta}^c \, dz + i$$

where: L = length of the high hydraulic conductivity soil layer, here fixed on 1 meter

$\overline{\Theta} = \frac{1}{L}\int_0^L \overline{\theta} \, dz$, the average moisture content over a vertical profile with length L

K_s = saturated hydraulic conductivity

β = slope of the plain (grid element)

$\overline{\theta}$ = reduced moisture content $(\theta - \theta_r)/(\theta_s - \theta_r)$, reaching from 0 till 1 (see sub-paragraph 5.4.1)

c = a pore size distribution factor, which will be a constant

i = input from rainfall

Equation (6.1) has been obtained starting from the Brooks and Corey (1964) relationship between hydraulic conductivity and moisture content (see paragraph 5.4.1). Moreover in equation (6.1) the kinematic hypotheses has been inserted. This leads to the following expression for the downslope flow:

$$(6.2) \quad q = \int_0^L K(\bar{\theta}) \tan\beta \, dz$$

where q is the horizontal downslope flux, $K(\bar{\theta})$ is hydraulic conductivity at reduced moisture content $\bar{\theta}$, L is the depth in z direction of the grid cell and tanβ is the slope angle with the horizontal.
With the use of a technical computing environment for high-performance numeric computation and visualisation called MATLAB, it is found that for a certain number of profiles a $c1$ and c2 value can be found such that:

$$(6.3) \quad \bar{\Theta}^{c1} \approx \frac{1}{L} \int_0^L \bar{\theta}^{c2} dz$$

where $c1$ and $c2$ are parameters to be fitted.
Starting from above mentioned hypothesis equation (6.1) may be rewritten as:

$$(6.4) \quad L(\theta_s - \theta_r) \frac{\partial \bar{\Theta}}{\partial t} = -K_s \tan\beta \, L \frac{\partial \bar{\Theta}^{c1}}{\partial y} + i$$

Equation (6.4) will be solved with the method of the characteristics as will be shown in the following subparagraph.

6.3 Computing experiments

The analytical solution of the kinematic wave by the method of characteristics has two main advantages over numerical solutions. It eliminates the wave celerity damping and phase lag, usually induced by numerical schemes and in addition, results in faster computational procedures (Borah et al., 1980). In spite of these advantages, applications of this analytical solution have been restricted in the past to catchment models with a high degree of geometric abstraction. One of the reasons is the formation of kinematic shock waves.

In a layer with a high hydraulic conductivity it can be assumed that vertical propagation will take place with a time delay that is negligible with respect to the horizontal propagation delay. A vertical equilibrium profile is therefore quickly established (see paragraph 5.4). Consequence of this assumption is that saturation will start from the bottom of the first layer. While accumulating on the bottom of the first layer lateral subsurface runoff will occur due to gravity forces caused by the angle of the hillslope with the horizontal.

The basic idea of a higher conductivity in the first layer of limited dimension (the rootzone) in TOPMODEL, is stated by Freeze (1972b), and Sloan and Moore (1984). The solution given here will maintain this statement. However, the exponential decay in which this phenomena is presented in TOPMODEL (see figure 5a,b) will be replaced by an equation that gives the relation of hydraulic conductivity with moisture content while neglecting dependence of saturated hydraulic conductivity with depth. This means that we will consider a vertical layer of limited dimensions characterised by a high constant saturated conductivity, but with a correspondent hydraulic conductivity varying upon moisture content.
TOPMODEL doesn't explicitly state this relation, but considers a correlation between z and transmissivity (see footnote 2 in paragraph 4.3). This relationship between K and θ is taken from Brooks and Corey (1964) (as derived in paragraph 5.4.1), and is based on extensive laboratory study of porous media, which indicates that, quite closely (Smith and Herbert, 1983):

$$(6.5) \quad K(\theta) = K_s \left[\frac{\theta - \theta_r}{\theta_s - \theta_r} \right]^{\varepsilon} = K_s \, \bar{\theta}^{\varepsilon}$$

in which

θ_r = residual value of θ, below which water cannot be extracted by capillary forces;

θ_s = saturated moisture content;

ε = a pore size distribution factor (in the case of Smith and Herbert (1983) typically from 3 to 4;

$\bar{\theta}$ = reduced moisture content $(\theta - \theta_r)/(\theta_s - \theta_r)$, reaching from 0 till 1.

The problem is that we do not really know the unsaturated profile in a catchment for which we want to simulate the rainfall-runoff response. This means we don't know the real $\theta(z)$. What we do know is the total moisture content (from the mass balance equation). So we simulated with the use of the numerical package MATLAB a number of profiles with variation of moisture content with depth of 1 meter. This 1 meter of unsaturated zone is generated from the article of Troch et al. (1993a). They concluded that variation in soil moisture is limited to the upper 1 meter layer, and that below this depth soil moisture content remains nearly constant and near field capacity throughout the

year. Besides that we presume an impermeable layer at 1 meter where no water is suppose to pass through in the time that runoff, as a consequence of rainfall, will occur.

6.3.1 Flux produced with different moisture content

In total fifty-eight different profiles of moisture content with depth are calculated. These fifty-eight artificial profiles can be divided in twelve groups of equal total reduced moisture content. The twelve different groups are: $\overline{\theta} = 0.0438$, $\overline{\theta} = 0.1375$, $\overline{\theta} = 0.2375$, $\overline{\theta} = 0.2750$, $\overline{\theta} = 0.3125$, $\overline{\theta} = 0.4125$, $\overline{\theta} = 0.4500$, $\overline{\theta} = 0.4875$, $\overline{\theta} = 0.5875$, $\overline{\theta} = 0.7125$, $\overline{\theta} = 0.8125$ and finally $\overline{\theta} = 0.9375$. Each group has four profiles that differ in shape but have, as mentioned above, all the same total reduced moisture content.
The first twelve profiles are shown in appendix 12, where the idea is to have a lower moisture content in the top of the profile and a higher at the bottom, with a transition phase from 0.5 till 0.75 meter below surface. It should be notified that due to the inability of the MATLAB drawing utility, the *z*-axis which represents the depth, is not expressed in the vertical axis, as would be expected, but in the horizontal axis.
The second twelve profiles are shown in appendix 13, where the idea is to have the same profile of moisture content in the first 0.5 meter but in addition to change the transition phase and finally adjust the rest of the profile to get the final same total moisture content groups as mentioned above.
The third twelve profiles are shown in appendix 14 and they represent the inverse profiles of appendix 12.
The fourth twelve profiles are shown in appendix 15, where the idea is to have the same shape in the bottom of the profile, from 0.75 m. till 1 m., as in appendix 12, but in addition vary the transient phase from 0 m. till 0.75 m.
Finally ten extra profiles have been taken into account as shown in appendix 16. These ten profiles differ in two ways from those shown in appendix 12 till appendix 15. First of all the total moisture content varies. They are for the ten profiles respectively: $\overline{\theta} = 0.1000$, $\overline{\theta} = 0.2013$, $\overline{\theta} = 0.2988$, $\overline{\theta} = 0.4010$, $\overline{\theta} = 0.4995$, $\overline{\theta} = 0.4998$, $\overline{\theta} = 0.6015$, $\overline{\theta} = 0.7488$, $\overline{\theta} = 0.8000$, $\overline{\theta} = 0.8763$. And second is the idea of having an extreme low moisture content at the top of the profile and a high moisture content at the bottom of the profile. This is to study the effect as we described caused by macropores (see Beven and Germann, 1982). The transition phase is varying from 0.1 till 0.75 meter below surface.

For all this fifty-eight profiles we calculated the flux (q) in the horizontal direction and compared these results with the flux calculated with the average value of moisture content in the profiles ($\overline{q}$), with the below mentioned equation:

$$\overline{q} \approx q$$

$$\int_0^L K_s\, \overline{\Theta}^{c1} \tan\beta \, dz \approx \frac{1}{L} \int_0^L K_s\, \overline{\theta}^{c2} \tan\beta \, dz \tag{6.6}$$

where $\bar{q}$ = the flux index calculated with the average moisture content
q = the flux index calculated with the point by point moisture content

With the use of MATLAB we fitted the constants $c1$ and $c2$, so that $\bar{q} \approx q$. For the values $c1$ = 3.25 and $c2$ = 10 the figure as shown in appendix 17 appears, see also table 3.1 for calibrated values.
As we can see in appendix 17 the result is quite satisfying. The uninterrupted line (with points on it) presents the flux calculated with the know total average moisture content over the profile of 1 meter. The rest of the profiles (in total fifty-eight) are presented as points using +, ., o, x, and *. As we can see the forty-eight profiles as shown in appendices 12 till 15 (respectively +, ., o and x) give a lower flux than then the once calculated with the average moisture content (uninterrupted line with points on it). An important prove is delivered by flux produced by appendix 12 and 14. They prove to be exactly the same. Hereby we can conclude that considering the different shapes of profiles, equation (6.6) gives the same results for inverse profiles with the same moisture content. There is another trend to be read from these point as the follow almost parallel to the average moisture content. A consequent divergent result is given for the calculations made with moisture content $\bar{\theta}$ = 0.7125. No physical or mathematical explanation however can be given for this behaviour. A further point to be noticed in the results shown in appendix 17 is that until moisture content $\bar{\theta}$ = 0.4125, no significant flow is calculated. Physically this can very well be explained considering the fact that some water has to be available in the profile before runoff occurs. As a consequence it is hereby shown that indeed flux will occur even when complete saturation is not reached as yet (note that saturation is reduced moisture content with value 1).
The ten extra profiles with a different total moisture content than the forty-eight discussed above, show a same trend in producing flux. It is remarkable that the flux is in general higher than the once calculated with the average moisture content (uninterrupted line with points on it). A physical explanation could be the fact that a higher moisture content in the bottom of the profile (see appendix 16) combined with a higher hydraulic conductivity and therefore transmissivity at that place produces a higher flux or horizontal runoff in the unsaturated zone. It is also remarkable that flux occurs in an earlier stage. After $\bar{\theta}$ = 0.2013, a flux is calculated already which rapidly increases as moisture content rises.

It can be concluded that a general trend exist that shows the increasing of flux with increasing moisture content both calculated with the average moisture content of a profile as well as the point by point moisture content. This could be a great step forward in simplifying physically based rainfall-runoff models. Instead of having the knowledge about the real profile, the integral moisture content of a profile can be sufficient enough to describe the resulting flux (by means of the kinematic wave approximation) in the unsaturated zone. An exact knowledge of the profile-shape is therefore no longer needed to describe the physical process of runoff.

However the resulting higher flux index produced by the ten extra profiles as shown in appendix 16, gave rise to an other approach of the process of hydraulic conductivity with moisture content and resulting flux, as will be discussed in the next subparagraph.

6.3.2 Comparison of van Genuchten expression with our analytical derivation

The relation of hydraulic conductivity with moisture content as described by van Genuchten in sub-paragraph 5.4.1, will be compared with an analytical derivation of hydraulic conductivity with moisture content, that takes the integral values into account instead of the point by point values, as described in appendix 11. Again a number of artificial profiles are taken into account (eleven this time). In contrast with the profiles mentioned in sub-paragraph 6.3.1, these eleven profiles do not have the exact same total moisture content as the eleven they have been compared with. Or more exact, the aim is to compare them and see if it is possible to fit them with some parameters even if they don't have exactly the same total moisture content, which is a different approach of the problem.

The aim of this part of the research is to show that the reduced moisture content with depth and the increasing hydraulic conductivity (and therefore transmissivity) with depth, can be described in the same way as van Genuchten does, by our analytical expression, using integral values instead of point by point values. By fitting a few parameters the two above mentioned processes can be described, again without knowing the real shape of the profile but only the saturated hydraulic conductivity and the initial reduced moisture content $(\overline{\theta}_0)$.

The resulting graphs made by calculating within MATLAB are shown in appendices 18 till 22. Appendix 18 shows the results of calculating reduced moisture content with depth both with van Genuchten expression (see equation (5.3)) and with our expression (see equation (11.4)). As we can see they have fairly well the same shape, although the area under the lines (the total moisture content) is not exactly the same. Appendix 19 shows the results of calculating total moisture content by van Genuchten (see equation (5.3)) and with our expression (see equation (11.7.2)). The fact that the total moisture content is not the same is shown here. Appendix 20 shows the results of calculating hydraulic conductivity with depth by van Genuchten (see equation (5.6)) compared with our expression of hydraulic conductivity with depth (see equation (11.9)). Again these lines show more or less the same shape. Appendix 21 shows the results of calculating transmissivity by van Genuchten (see equation (5.6)) compared with transmissivity calculated by our expression (see equation (11.13)). This graph shows that the transmissivity with depth is practically the same even though we know the total moisture content is not the same. Since we work with centimetres in these calculations the y-axis of appendix 20 is multiplied by a hundred in appendix 21 and 22. Finally in appendix 22 the most important plot of this part of the research is shown. Appendix 22 shows the comparison of the description of increasing transmissivity (end therefore flux), with increasing moisture content, both calculated with van Genuchten expression and our

expression. The dashed-dotted line presents the van Genuchten equations (5.3) against (5.6) and the uninterrupted line presents our equations (11.7.2) on the x-axis against (11.3) on the y-axis. The relative distance between the lines compared to the total transmissivity reaches from 0 % in the top till a maximum of 9.82% in the centre were the soil is filled with 50% of water. This distance can be reduced by refitting the parameters as mentioned in table 3.2. However it is shown that the same process of increasing transmissivity can also be described by not knowing the shape of the profile but only the total moisture content in the unsaturated profile of the first meter of soil.

The ten lines in appendix 18 and 20 produce eleven profiles, because the eleventh profile is the one completely filled with water (saturated profile). Looking at appendix 20 we see that the maximum value of hydraulic conductivity is 0.02 cm/s (0.72 m/hr.). In the case of these calculations hydraulic conductivity is just another parameter which changes has no effect on the shape of the graphs shown in appendix 20 and 21 but will only change the values of the y-axis. However the value of hydraulic conductivity obtained, is carefully chosen from literature. Beven (1981) gives in his article about kinematic subsurface storm flow a table with an overview of studies being performed on subsurface storm flow that also mentions different values of saturated hydraulic conductivity. The value 0.02 cm/s is a careful chosen average of the values mentioned in that table.

Appendices 19, 21 and 22 show that although the moisture content is not exactly the same the transmissivity produced by these different profiles is nearly the same. The plotted values of these appendices are also printed in the table below:

Appendix 22				
Appendix 19			Appendix 21	
depth of the profiles	moisture content van Genuchten	moisture content our expression	transmissivity van Genuchten	transmissivity our expression
	%	%	(cm^2/s)	(cm^2/s)
100 cm.	16.8089	17.0488	0.0121	0.0269
90 cm.	21.0549	26.9006	0.2000	0.2267
80 cm.	28.4701	36.5355	0.4000	0.4262
70 cm.	36.6885	45.9320	0.6000	0.6254
60 cm.	45.2917	55.0630	0.8000	0.8242
50 cm.	54.1264	63.8934	1.0000	1.0225
40 cm.	63.1180	72.3755	1.2000	1.2204
30 cm.	72.2239	80.4400	1.4000	1.4175
20 cm.	81.4173	87.9757	1.6000	1.6138
10 cm.	90.6803	94.7661	1.8000	1.8087
0 cm.	100.0000	100.0000	2.0000	2.0000

Table 6a The different values for reduced moisture content and transmissivity with depth, calculated with the van Genuchten expression and our expression. Results are also printed in appendix 19 ,21 and 22.

The appendices 18 and 20 can not immediately be compared with appendices 19 and 21, since different equations are compared in each graph (see expatiation above). However in appendix 22 a comparison is made that shows the effect of increasing moisture content on the transmissivity of the soil. The lines are not exactly the same but that could be caused by the fact that the total moisture contents are not exactly the same as shown in appendix 19. It is obvious however that the process calculated with the point by point value of moisture content (as van Genuchten does) or the integral (or total) moisture content of the profiles (as in our expression) or almost similar. This appendix 22 can be compared with appendix 10 and appendix 17, as the all show the same process, with different soil characteristics however. Making this comparison it is remarkable that appendix 22 shows less concave lines, in fact the van Genuchten line is even a bit convex. This can be (as discussed) explained by the obtained values of the parameters as shown in table 3.2.

Again is shown that it is possible of describing the process by not knowing the exact shape of the profile but only the total or integral value of the profile. This last mentioned result is a great step forward in using a new lumped parameterization for describing transmissivity in the unsaturated zone and therefore describing the process of runoff in a catchment without knowing the real shape of the profiles. This new technique can be used in topographic based rainfall-runoff models, by using a "flux index curve" that gives runoff on the bases of integral moisture content of the profile instead of the real shape of the profile. An other, more physically correct way, of showing flow routing in an unsaturated subsurface layer is hereby introduced. This method can be applied into the TOPMODEL, which was subject of extensive study in this report, but also in other (topographical based) rainfall-runoff models.

7. CONCLUSIONS

Ever since the beginning of rainfall-runoff modelling the aim for hydrologists was to try to create physically based models with structural simplicity. In 1979, Beven and Kirkby developed TOPMODEL, a hydrological forecasting model combining, a dynamic contributing area model based on $\ln(a/\tan\beta)$ (the topographic index), the channel network topology, and a simple lumped parameter basin routing model. The model parameters were physically based in the sense that they may be determined directly by measurements. Using only estimated and measured parameter values the model made satisfactory predictions of catchment response. This is shown by Wood et al. (1988), Durand et al. (1992), Troch et al. (1993a,b), Franchini et al. (1993) and finally also in this report by a small experiment on a sub-catchment of the Reno river. Franchini et al. (1993) report that the model is surprisingly insensitive to the actual basin's index curve. Therefore its is possible to use it without the calibration process for this topographic index curve which makes the TOPMODEL even more applicable compared with other rainfall-runoff models.

There are however some problems in the physical meaning of the calibrated parameters in the TOPMODEL, and in the way some physical processes are described. First of all there is an artificial high hydraulic conductivity which systematically increases with the increasing grid size of the DTM. Since TOPMODEL implies a steady state assumption, there is no time delay in transporting water from one upstream end of the grid to the downstream one. With increasing grid sizes from 25 till 400 meter this hypotheses looses his value. The second problem is that as a result of this phenomenon the TOPMODEL in practical applications, denies the possibility of representing the surface runoff formation process from infiltration excess, since no Hortonian process will take place. In fact all the runoff will occur in saturated conditions. Many authors however stated that flow in the unsaturated zone of a catchment is of significant importance (Freeze, 1972b; Sloan and Moore, 1984; Stagnitti et al., 1986). Besides that Beven and Germann (1982) state that macropores and other structural channels in the rootzone give not only rise to a high hydraulic conductivity but also to a lateral flow in the unsaturated zone on a hillslope.

To solve the above mentioned problems in TOPMODEL, but also in other topographical rainfall-runoff models, a simple water routing model in the unsaturated zone can be used. The kinematic wave approximation combined with the Brooks and Corey (1964) equations of describing hydraulic conductivity with moisture content seems to be appropriate. The depth of the soil with a high hydraulic conductivity (caused by macropores) will be negligible with respect to the horizontal grid dimensions. This allows the transient phase of vertical propagation to be neglected. A further simplification is introduced by making reference to the integral value of the vertical moisture content, instead of the real vertical equilibrium profile.

With the use of MATLAB, forty-eight profiles are calculated to produce flux using only there integral value of reduced moisture content. The are compared and fitted with twelve profiles where the flux is calculated from the point by point values of moisture content. It can be concluded that a general trend exist that shows the increasing of flux with increasing reduced moisture content, as shown in appendix 17. Remarkable is that the inverse profiles as shown in appendix 12 and 14 give the exact same flux. These above mentioned results could be a great step forward in simplifying physically based rainfall-runoff models. Instead of having the knowledge about the real profile, the integral moisture content of a profile can be sufficient enough to describe the resulting flux (by means of the kinematic wave approximation) in the unsaturated zone. An exact knowledge of the profile-shape is therefore no longer needed to describe the physical process of runoff. Ten extra profiles with an extreme low moisture content in the top of the profile and a high moisture content in the bottom with a different total moisture content as the profiles mentioned above are also compared. They produce a higher flux than the point by point calculated profiles. This can be explained by the fact that a higher moisture content in the bottom of the profile (see appendix 16) combined with a higher hydraulic conductivity produces a higher flux or horizontal runoff in the unsaturated zone. It seams that not all thinkable shapes of the profiles are physically acceptable. This last result gave rise to a more in depth analyse of the problem.

The aim of the sequel research was to show that the reduced moisture content with depth and the hydraulic conductivity with depth, can be described in the same way as van Genuchten does, by an analytical expression which allows to make use of integral values instead of point by point values (see appendix 11). By fitting a few parameters the two above mentioned processes could be described, again without knowing the real shape of the profile.

Although it is shown that the total reduced moisture content in the eleven compared profiles of appendix 18 till 22 is not exactly the same, the resulting transmissivity with depth is practically the same. The results of calculating transmissivity with different moisture contents is shown in appendix 22. It shows that there is an order of 9.82% maximum difference. By refitting the parameters in getting the same moisture content this difference will vanish. It is shown in this doctoral thesis that there exist a way of describing transmissivity (or hydraulic conductivity or flux index), both with the point by point moisture content as well as with only the total or integral value of reduced moisture content of the profile. This last prove is the most important conclusion of this research. It shows that there is way of describing runoff in the unsaturated zone with kinematic wave approximation by taking only the integral reduced moisture content into account This result can be used by means of a "flux index curve" in topographical based rainfall-runoff models such as the TOPMODEL as well as in other topographical based rainfall-runoff models.

ACKNOWLEDGEMENTS

I would like to thank Prof. Ezio Todini and Dott. Ing. Patrizia Di Giammarco for the supervision and support they gave me in writing this doctoral thesis. Especially Dottoressa Patrizia Di Giammarco was very patiently with me and always managed to get me back on the right track. I also like to thank Prof. J. J. Bogardi for his supervision and the useful and correcting notes given on the draft of this paper.

This work was done with the fund of a European Community Erasmus scholarship and by funds provided by the department of Hydraulic Construction from the University of Bologna.

Last but not least I would like to thank all the friends I made during my stay in Italy. Not only did they encourage me to learn the Italian language, but by their appearance made my stay in the beautiful city of Bologna an unforgettable phase of my life.

Ronald Benning

REFERENCES

Abbott, M.B., Bathurst, J.C., Cunge, J.A., O'Connell, P.E. and Rasmussen, J., 1986a. An introduction to the European Hydrological System - Système Hydrologique Européen, "SHE", 1: History and philosophy of a physically-based, distributed modelling system. J. Hydrol., 87: 45-59.

Abbott, M.B., Bathurst, J.C., Cunge, J.A., O'Connell, P.E. and Rasmussen, J., 1986b. An introduction to the European Hydrological System - Système Hydrologique Européen, "SHE", 2: Structure of physically.based, distributed modelling system. J. Hydrol., 87: 61-77.

Abdul, A. S., and R. W. Gillham, 1984. Laboratory studies on the effect of the capillary fringe on streamflow generation. Water Resour. Res., 20(6), 691-698.

Amorocho, J. and G.T. Hurt, 1964. Nonlinear analysis of hydrologic systems, Water Resour. Res. Contrib. 40, University of California, Berkeley.

Anderson, M.G. and T.P. Burt, 1985. Hydrological forecasting. John Wiley & Sons Ltd., Chichester-New York-Brisbane-Toronto-Singapore.

Bacchi, B., Burlando, P., Rosso, R. and Todini, E., 1986. Hydrological models for real time flood forecasting. Proc. Int. Conf. Arno Proj., Florence CNR-CNDCI, Rep. 29.

Bathurst, J.C. 1986. Physically based distributed modelling of an upland catchment using the Systeme Hydrologique Europeen, Journal of Hydrology 87 pp. 79-102.

Beven, K.J. and Kirkby M.J., 1979. A physically based, variable contributing area model of basin Hydrology. Hydrological Sciences-Bulletin des Sciences Hydrologiques, 24, 1-3.

Beven, K.J., 1981. Kinematic subsurface stormflow, Water Resour. Res., Vol. 17 no. 5, pp. 1419-1424.

Beven, K.J., 1982. On subsurface stormflow: Predictions with simple kinematic theory for saturated and unsaturated flows, Water Resour. Res., Vol. 18 no. 6, pp. 1627-1633.

Beven, K.J. and P. Germann, 1982. Macropores and water flow in soils, Water Resour. Res., Vol. 18, no. 5, pp. 1311-1325.

Beven, K.J., 1984. Infiltration into a class of vertically non-uniform soils, Hydrological Sciences Journal, Vol. 29 no.4, pp. 425-434.

Beven, K.J., 1986a. Runoff production and flood frequency in catchments of order n: An alternative approach, in: Scale problems in Hydrology, edited by V.K. Gupta, I. Roderigues-Iturbe and E.F. Wood , D. Reidel, Hingham, Mass..

Beven, K.J. 1986b. Hillslope runoff processes and flood frequency characteristics, in Hillslope Processes, edited by A.D. Abrahams, Allen and Unwin, Winchester, Mass..

Beven, K.J., A. Calver and E.M. Morris, 1987. The Institute of Hydrology Distributed Model (IHDM). Inst. Hydrolo. Rep. no.98, Wallingford.

Beven, K.J., Wood E.F., and Sivapalan M., 1988. On hydrological heterogeneity-catchment morphology and catchment response. Journal of Hydrology, 100, pp. 353-375.

Beven, K.J., 1989. Changing ideas in hydrology - The case of physically-based models, Journal of Hydrology, 105, pp. 157-172.

Binley, A., J. Elgy and K.J. Beven, 1989. A physically based model of heterogeneous hillslopes 1. Runoff production, Water Resour. Res. Vol. 25, no. 6, pp. 1219-1226.

Borah, D.K., S.N. Prasad and C.V. Alonso, 1980. Kinematic wave routing incorporating shock fitting, Water Resour. Res. Vol. 16, no. 3, pp. 529-541.

Brooks, R.H. and A.T. Corey, 1964. Hydraulic properties of porous media, Hydrol. Pap. 3, Colo. State Univ., Fort Collins.

Burnash, R.J.C., Ferral, R.L. and McGuire, R.A., 1973. A general streamflow simulation system Conceptual modelling for digital computers. Report by the Joint Federal State River Forecasts Center, Sacramento, Calif.

Charbeneau, R.J., 1984. Kinematic models for soil moisture and solute transport, Water Resour. Res., Vol. 20, no. 6, pp. 699-706.

Chow, V.T., D.R. Maidment, and L.W. Mays, 1988. Applied Hydrology. McGraw-Hill Intern. Editions, Singapore.

Cordova, J.R., I. Roderiguez-Iturbe, 1983. Geomorphologic estimation of extreme flow probabilities, Journal of Hydrology 65, pp. 159-173.

Crawford, N.H. and Linsley, R.K., 1966. Digital simulation in hydrology, Stanford watershed model IV. Tech. Rep. No. 39, Dep. Civ. Eng., Stanford University.

Dawdy, D.R. and O'-Donnel, T., 1965. Mathematical models of catchment behauviour. J. Hydraul. Div., Proc. ASCE, HY4.

Dooge, J.C.I., 1957. The Rational Method for Estimating Floot Peak. Engineering (Londen), 184: 311-3374.

Dooge, J.C.I., 1973. The linear theory of hydrologic systems. Tech. Bull.U.S. Dep.Agric., No. 1468, U.S. Gov. Print. Off., Washington, D.C.

Dunne, T., T.R. Moore, and C.H. Taylor, 1975. Recognition and prediction of runoff-producing zones in humid regions, Hydrol. Sci. Bull., vol. 20, no. 3, pp. 305-327.

Dunne, T. 1978. Field studies of hillslope flow processes, in Hillslope Processes, edited by M.J. Kirby, pp. 227-293, John Wiley, New York.

Durand, P., Robson A., and Colin N., 1992. Modelling the hydrology of submediterranean montane catchments (Mont-Lozère, France) using TOPMODEL: intial results. Journal of Hydrology, 139 (1992) pp. 1-14.

Eagleson, P.S., 1970. Dynamic Hydrology, McGraw-Hill, New York.

Franchini, M. and M. Pacciani, 1991. Comparative analysis of several conceptual rainfall runoff models. Journal of Hydrology, 122 pp. 161-219.

Franchini, M., J. Wendling, E. Todini and Ch. Obled 1993. Physical interpretation and sensitivity analysis of the TOP Model, submitted to Journal of Hydrology.

Freeze, R.A. and R.L. Harlan, 1969. Blueprint for a physically based digitally simulated hydrologic response model, Journal of Hydrology no. 9, pp. 237-258.

Freeze, R.A., 1972a. Role of subsurface flow in generating surface runoff, 1, Base flow contributions to channel flow, Water Resour. Res., 8 (3), 609-623.

Freeze, R.A., 1972b. Role of subsurface flow in generating surface runoff, 2, Upstream sourch areas, Water Resour. Res., 8 (6), 1272-1283.

Freeze, R.A., 1980. A stochastic-conceptual analysis of rainfall-runoff processes on a hillslope, Water Resour. Res., Vol. 16 no. 8, pp. 1272-1283.

Green, W.H. and G.A. Ampt, 1911. Studies on soil physics, part I, the flow of air and water through soils, J. Agric. Sci., Vol. 4 no. 1, pp. 1-24.

Gupta, V.K., I. Rodriguez-Iturbe, and E.F. Wood, 1986. Scale problems in hydrology. Water science and technology library, D. Reidel Publishing Company, Dordrecht, Holland.

Henderson, F.M., R.A. Wooding, 1964. Overland flow and groundwater flow from a steady rainfall of finite duration, Journal of Geophysical Research, Vol. 69, no. 6 pp. 1531-1540.

Horton, R.E., 1933. The role of infiltration in the hydrologic cycle. Trans. Am. Geophys. Union, Vol. 14, pp. 446-460.

Horton, R.E., 1939. Analysis of runoff plat experiments with varying infiltration capacity, Trans. Am. Geophys. Union, Vol. 20 pp. 693-711.

Hurley, D.G. and G. Pantelis, 1985. Unsaturated and saturated flow through a thin porous layer on a hillslope, Water Resour. Res., Vol. 21, no. 6, pp. 821-824.

Keulegan, G.H., 1945. Spatially varied discharge over a sloping plane. Amer. Geophys. Union Trans. Part 6, pp. 956-959.

Kirkby, M.J., 1985. Hillslope hydrology, in Hydrological Forecasting, edited by M.G. Anderson and T.P. Burt, John Wiley & Sons Ltd.

Lighthill, F.R.S. and G.B. Whitham, 1955. On kinematic waves, I, Flood measurements in long rivers. Proc. Royal Soc. of Londen, A, 229, pp. 281-316.

Moore R.J. and R.T. Clarke, 1981. A distribution function approach to rainfall-runoff modeling, Water Resour. Res., Vol. 17, no. 5, pp. 1367-1382.

Moore R.J., 1985. The probability-distributed principle and runoff production at point and basin scales, Hydrological Sciences Journal, Vol. 30, no. 2, pp. 273-297.

Mosley, M.P., 1979. Streamflow generation in a forested watershed, New Zealand, Water Resour. Res., Vol. 15, no. 4, pp. 795-806.

Nash, J.E., 1958. The form of the instantaneous unit hydrograph, IUGG General Assembly of Toronto, Vol. III, Publ. n.45 - IAHS, Gentbrugge, pp. 57-64.

Nieber, J.L. and M.F. Walter, 1981. Two-dimensional soil moisture flow in a sloping rectangular region: Experimental and numerical studies, Water Resour. Res., Vol. 17, no. 6, pp. 1722-1730.

Philip, J.R., 1957. The theory of infiltration: 1. The infiltration equation and its solution, Soil Sci., Vol. 83, no. 5, pp. 345-357.

Quinn, P., K. Beven, D. Morris and R. Moore, 1991. The use of Digital Terrain Data in Modelling the Response of Hillslopes and Headwaters, Internal technical report, University of Lancaster.

Raudkivi, A.J., 1979. Hydrology, Pergamon Press, Oxford.

Richards, L. A., 1931. Capillary conduction of liquids through porous mediums, Physics, Vol. 1. pp. 318-333.

Rocwood, D.M. and Nelson, M.L., 1966. Computer application to streamflow synthesis and reservoir regulation. IV Int. Conf. Irrig. Drain.

Saint-Venant, Barre de, 1871. Theory of unsteady water flow, with application to river floods and to propagation of tides in river channels, French Academy of Science, Vol. 73, pp. 148-154, 237-240.

Sherman, L.K., 1932. Streamflow from rainfall by the unit graph method. Eng. News Rec., 108: 501-505.

Sivapalan, M.K., and Wood E.F., 1986. Spatial heterogeneity and scale in the infiltration response of catchments. Scale Problems in Hydrology, edited by V.K. Gupta, I. Rodriguez-Iturbe, and E.F. Wood, D. Reidel, Dordrecht, Holland, pp. 81-106.

Sivapalan, M., K. Beven and E.F. Wood, 1987. On Hydrologic Similarity 2. A Scaled Model of Storm Runoff Production. Water Resourch Research, Vol. 23 no. 12 pp. 2266-2278.

Sloan, G.P., I.D. Moore, 1984. Modeling subsurface stormflow on steeply sloping forested watersheds, Water Resour. Res., Vol. 20, no. 12, pp. 1815-1822.

Smith, R.E. and R.H.B. Hebbert, 1983. Mathematical simulation of interdependent surface and subsurface hydrologic processes, Water Resour. Res., Vol. 19, no. 4, pp. 987-1001.

Soil Conservation Service, 1972. SCS National Engineering Handbook, section 4, Hydrology, U.S. Department of Agriculture, Washington, D.C.

Stagnitti, F., M.B. Parlange, T.S. Steenhuis and J.-Y. Parlange, 1986. Drainage from a uniform soil layer on a hillslope, Water Resour. Res., Vol. 22, no. 5, pp. 631-634.

Steenhuis, T.S., J.-Y. Parlange, M.B. Parlange and F. Stagnetti, 1988. A simple model for flow on hillslopes, Agric. Water Manage., 14, pp. 153-168.

Stephenson, D. and M.E. Meadows, 1986. Kinematic Hydrology and Modeling, Developments in Water Science 26, Elsevier, Amsterdam.

Todini, E., A. Bossi.1986. PAB (Parabolic and Backwater) an unconditionally stable flood routing scheme particularly suited for real time forecasting and control. Journal of Hydraulic Research, Vol. 24, 1986, nod. 1993. A discussion about TOPMODEL.

Todini, E. 1988. Rainfall-runoff modeling past, present and future. Journal of Hydrology, 100 (1988) 341-352. Elsevier Science Publishers b.v.

Todini, E., Franchini M., 1988. PABL : a parabolic and backwater scheme with lateral inflow and outflow. 5 th IAHR Int. Symp. Stochastic Hydraulics, Birmingham, U.K.

Todini, E. 1989. Flood forecasting models. Excerpta, Vol 4, pages 117-162.

Troch, P.A., M. Mancini, C. Paniconi, and E.F. Wood, 1993a. Evaluation of a distributed catchment scale water balance model, Water Resour. Res., Vol. 29, no. 6, pp. 1805-1817.

Troch, P.A., J.A. Smith, E.F. Wood and F.P. de Troch, 1993b. Emperical and model based analysis of extreme flood events in a humid region, Extreme Hydrological Events: Precipitation, Floods and Droughts (Proceedings of the Yokohama Symposium, July 1993) IAHS Publ. no. 213, pp. 245-256.

van Genuchten, M.Th., 1980. A closed-form for predicting the hydraulic conductivity of unsaturated soils, Soil Sci. Soc. Am. J. no. 44, pp. 892-898.

Whipkey, R.Z, 1965. Subsurface stormflow from forested slopes, Int. Assoc. Sci. Hydrol. Bull., Vol. 10, no.2, pp. 74-85.

WMO, 1975. Intercomparison of Conceptual models used in operational hydrological forecasting. Oper. Hydrol. Rep. 7, WMO No. 429, Geneva.

Wood, E.F., M.Sivapalan, K.J. Beven and L. Band, 1988. Effects of spatial variability and scale with implications to hydrologic modeling, Journal of Hydrology, 102, pp. 29-47.

Woolhiser, D.A. and J.A. Ligget, 1967. Unsteady one-dimensional flow over a plane - The rising hydrograph. Water Resour. Res., Vol., 3 no. 3, pp. 753-771.

Zecharias, Y.B. and W. Brutsaert, 1988. Recession characteristics of groundwater outflow and base flow from mountainous watersheds, Water Resour. Res., Vol. 24, no. 10, pp. 1651-1658.

APPENDICES and TABLES

Appendix 1 Surface and sub-surface hillslope flow components (figure from: Hydrological Forecasting edited by M.G. Anderson and T.P. Burt, 1985)

Appendix 2 Mechanisms of runoff production
(figure form: Scale problems in hydrology edited by V.K. Gupta, I. Rodriguez-Iturbe and E.F. Wood, 1986)

Appendix 3 Infiltration by Horton's equation (figure from: Applied hydrology edited by V.T. Chow, D.R. Maidment and L.W. Mays, 1988)

Appendix 4 Variables in the Green-Ampt infiltration model. The vertical axis is the distance from the soil surface, the horizontal axis is the moisture content of the soil (figure from: Applied hydrology edited by V.T. Chow, D.R. Maidment and L.W. Mays, 1988)

Appendix 5 Schematic flow, q, from a catchment element draining into a 1-metre contour width: a = total area/ 1 m^2/ m. (figure from: Hydrological Forecasting edited by M.G. Anderson and T.P. Burt, 1985)

Appendix 6 Schematic representation of a valley and the formation of runoff according to the TOPMODEL: interflow (Q_b) and surface runoff (Q_s) from the contributing area A_c , where (S_i) is the total profile moisture deficit

Appendix 7 Map of the Reno river catchment in Italy with selected sub-catchment for TOPMODEL calibration and validation

Appendix 8 Output from the TOPMODEL for the calibration period February 1990 - May 1990

Appendix 9 Output from the TOPMODEL for the validation period June 1990 - December 1990

Appendix 10 The relation between soil hydraulic conductivity and water content (figure from: Smith and Hebbert, 1983)

Appendix 11 The analytical calculation of reduced moisture content with depth, integral moisture content with depth, hydraulic conductivity with depth and transmissivity (calculated by taking the integral value of moisture content) with depth

Appendix 12 First twelve profiles. With higher moisture content at the bottom than at the top. Transition-phase from 0.5 till 0.75 m. below surface

Appendix 13 Second twelve profiles. With changed transition form from 0.5 till 0.7 or 0.75 m.

Appendix 14 Third twelve profiles with lower moisture content at the bottom than at the top (reverse profiles from appendix 12). Transition from 0.25 till 0.50 m. below surface

Appendix 15 Fourth twelve profiles with varied forms of transition phase from 0 till 0.75 m.

Appendix 16 Ten extra profiles with an extreme low moisture content at the top of the profile and a high moisture content at the bottom of the profile. Transition is varying from 0.1 till .0.75 m. below surface.

Appendix 17 Compared flux index calculated with point by point moisture content or average moisture content

Appendix 18 Relation of reduced moisture content with depth calculated with van Genuchten equation (5.3) represented by (-.-.) and our equation (11.4) represented by (—)

Appendix 19 Percentage of soil filled with water calculated with van Genuchten equation (5.3) represented by (x), compared with our equation (11.7.2) represented by (0)

Appendix 20 Relation of hydraulic conductivity with depth calculated with van Genuchten equation (5.6) represented by (-.-.) and our equation (11.9) represented by (—)

Appendix 21 Transmissivity calculated with van Genuchten equation (5.6) represented by (x), compared with transmissivity calculated with our equation (11.13) represented by (o)

Appendix 22 Increasing transmissivity with increasing moisture content calculated with van Genuchten equations (5.3) and (5.6) represented by -.-. and calculated with our equations (11.7.2) and (11.3) represented by —

Table 1 The explained variance (EV), the determination coefficient (DC) and the correlation coefficient (CC) of both calibration period (February till May 1990) and validation period (June till December 1990). See TOPMODEL results in appendix 8 and appendix 9.

Table 2 Soil-level water balance component (TOPMODEL). Obtained parameter values of both calibration period (February till May 1990) and validation period (June till December 1990). See TOPMODEL results in appendix 8 and appendix 9.

Table 3.1 Calibrated values of parameters used to fit equation (6.6), as shown in appendix 17

Table 3.2 Calibrated values of parameters and soil characteristics used to fit van Genuchten equations with our equations as shown in appendices 18 till 22

Appendix 1 Surface and sub-surface hillslope flow components (figure from: Hydrological Forecasting edited by M.G. Anderson and T.P. Burt, 1985)

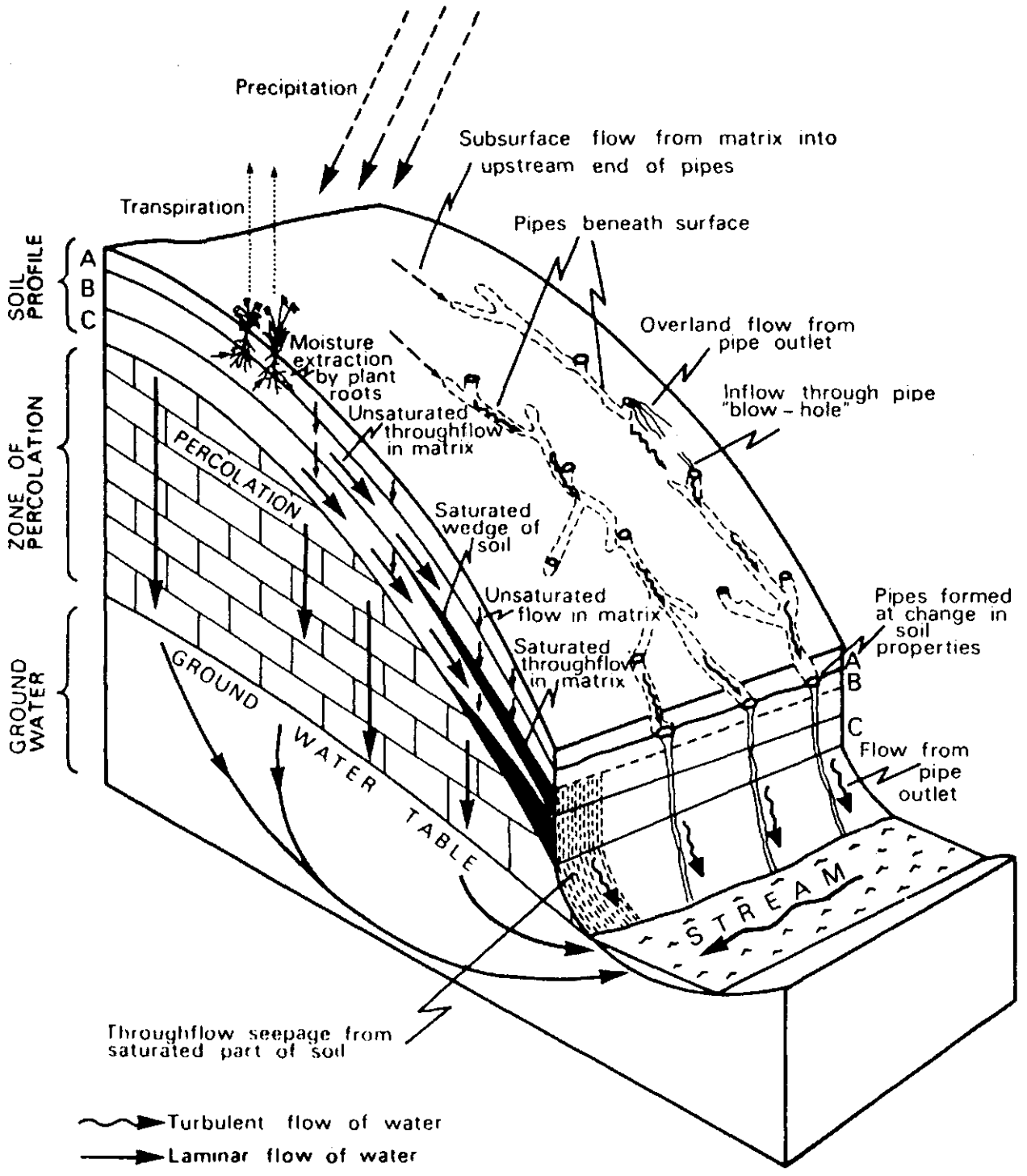

Appendix 2 Mechanisms of runoff production

P precipitation

P_C channel precipitation

f infiltration

of overland flow

rf return flow

if inter flow

wt water table

(figure form: Scale problems in hydrology edited by V.K. Gupta, I. Rodriguez-Iturbe and E.F. Wood, 1986)

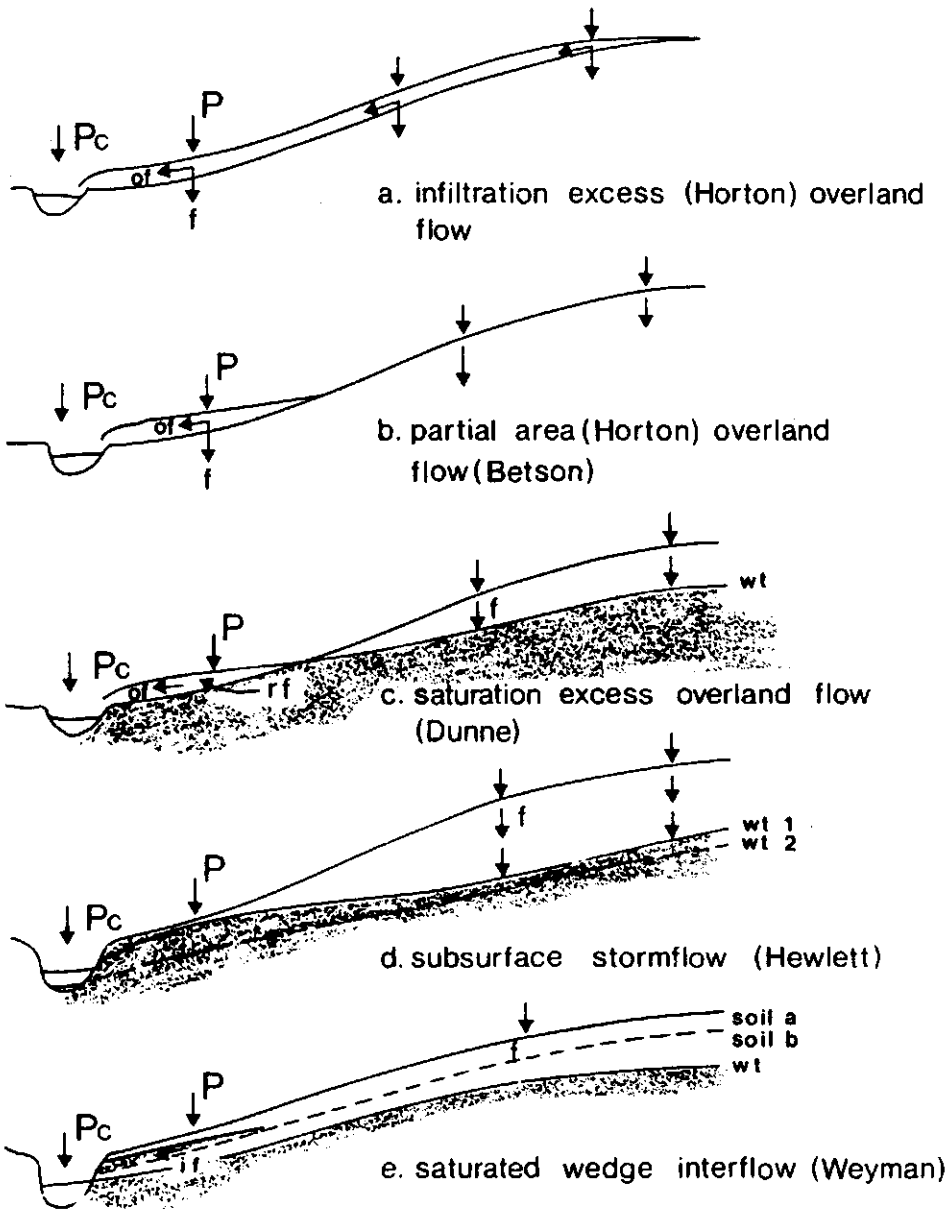

Appendix 3 Infiltration by Horton's equation (figure from: Applied hydrology edited by V.T. Chow, D.R. Maidment and L.W. Mays, 1988)

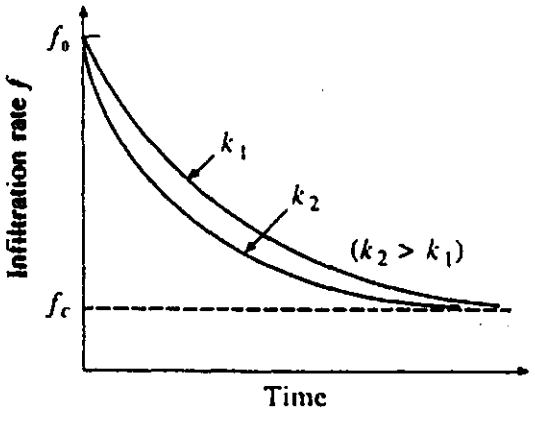

(*a*) Variation of the parameter k.

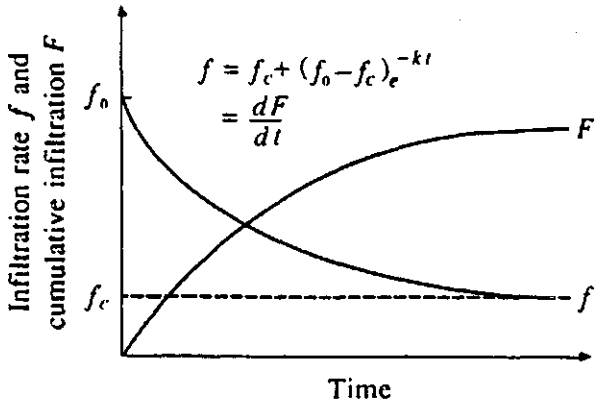

(*b*) Infiltration rate and cumulative infiltration.

Appendix 4 Variables in the Green-Ampt infiltration model. The vertical axis is the distance from the soil surface, the horizontal axis is the moisture content of the soil (figure from: Applied hydrology edited by V.T. Chow, D.R. Maidment and L.W. Mays, 1988)

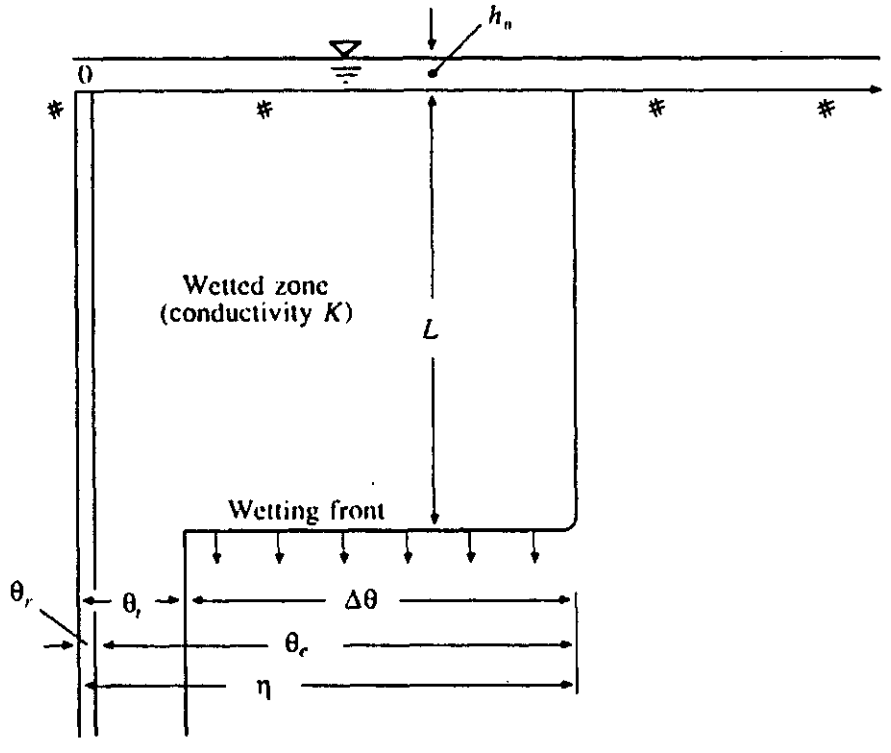

Appendix 5 Schematic flow, q, from a catchment element draining into a 1-metre contour width: a = total area/ 1 m^2/ m. (figure from: Hydrological Forecasting edited by M.G. Anderson and T.P. Burt, 1985)

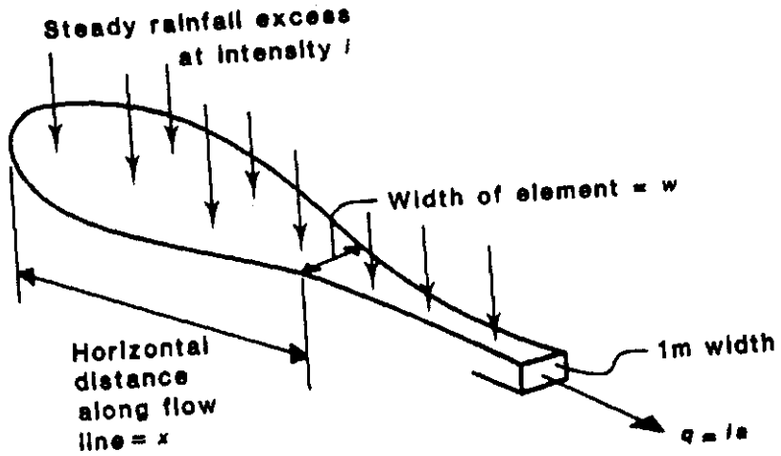

Appendix 6 Schematic representation of a valley and the formation of runoff according to the TOPMODEL: interflow (Q_b) and surface runoff (Q_s) from the contributing area A_c, where (S_i) is the total profile moisture deficit

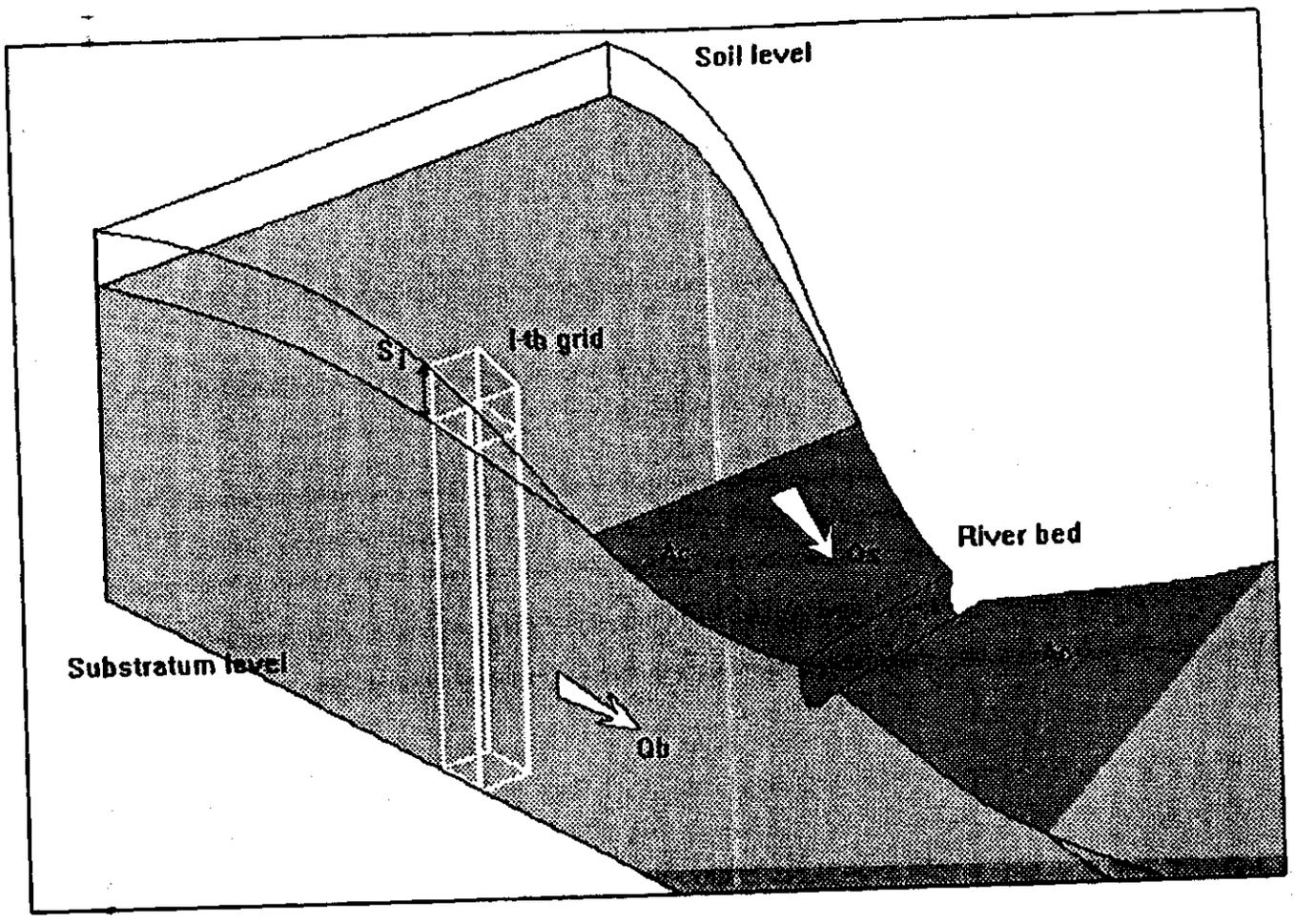

Appendix 7 Map of the Reno river catchment in Italy with selected sub-catchment for TOPMODEL calibration and validation

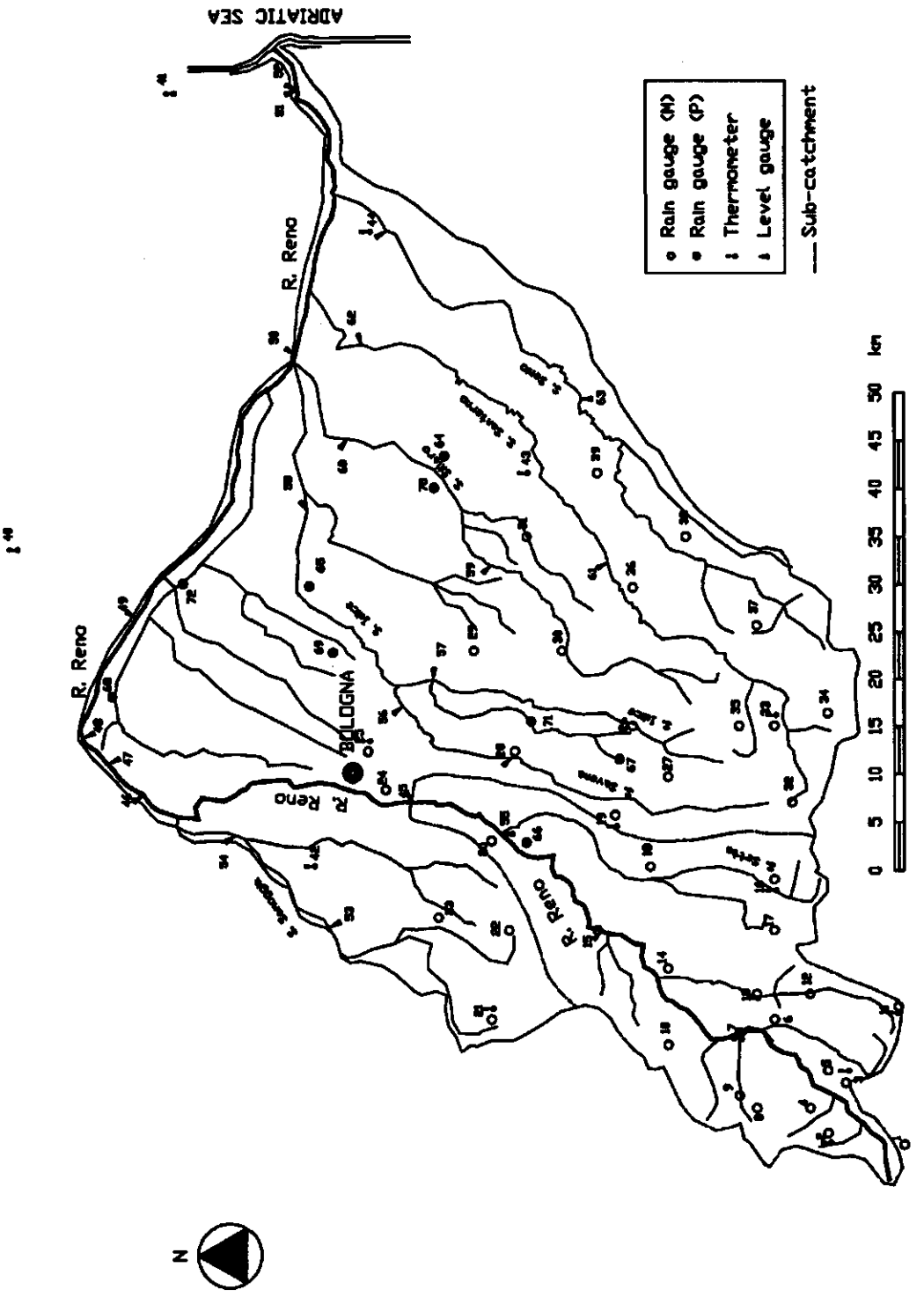

Appendix 8 Output from the TOPMODEL for the calibration period February 1990 - May 1990

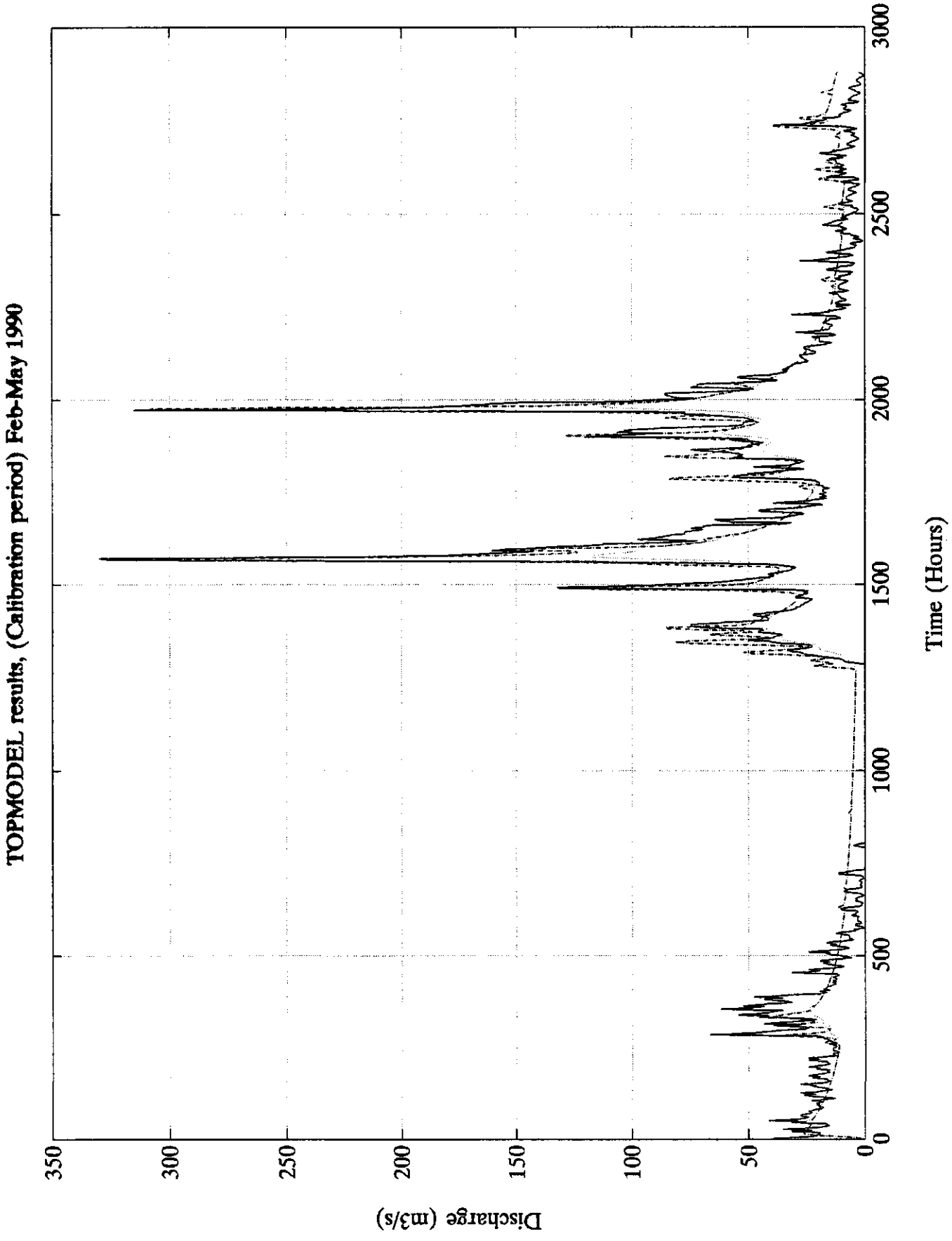

Appendix 9 Output from the TOPMODEL for the validation period June 1990 - December 1990

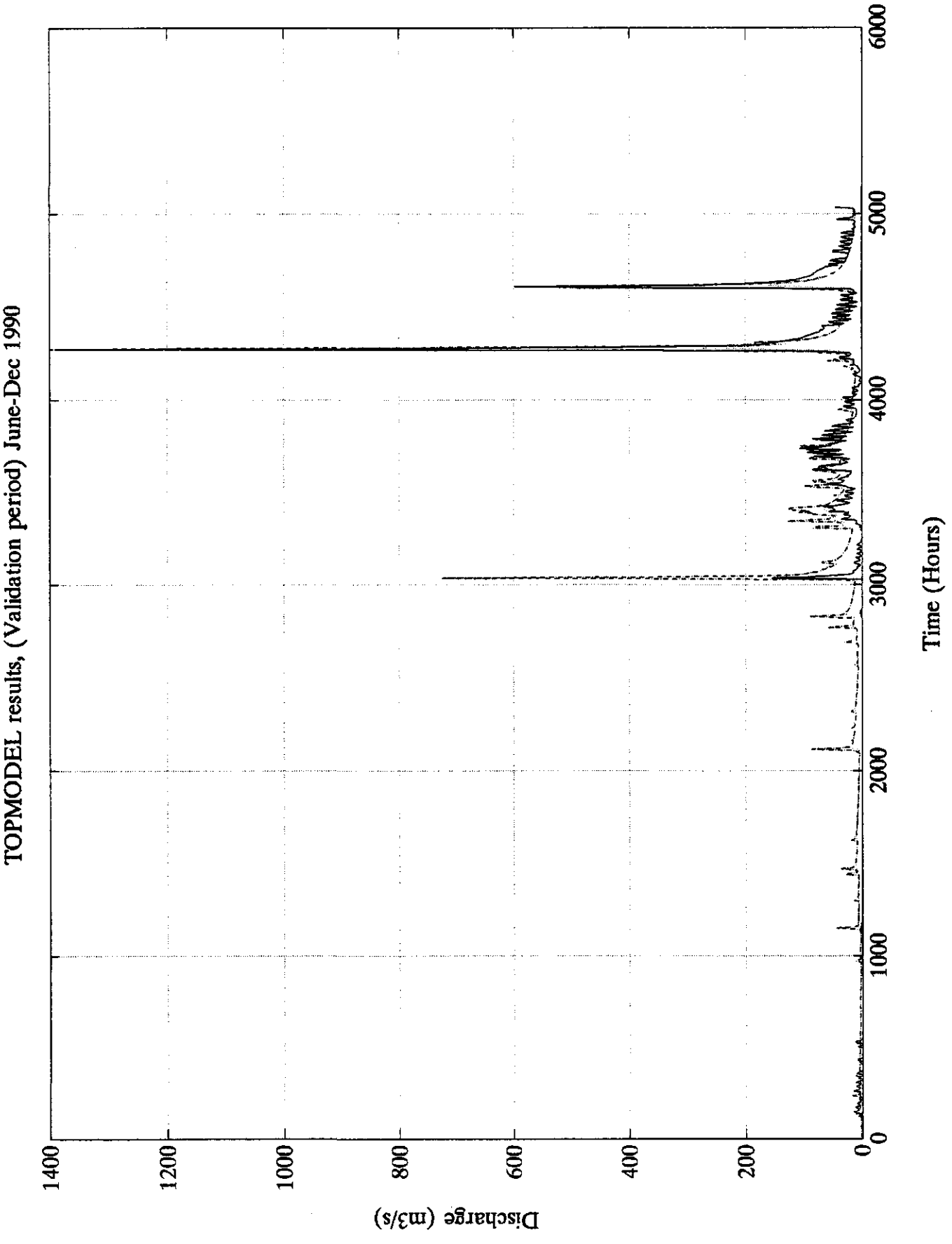

Appendix 10 The relation between soil hydraulic conductivity and water content (figure from: Smith and Hebbert, 1983)

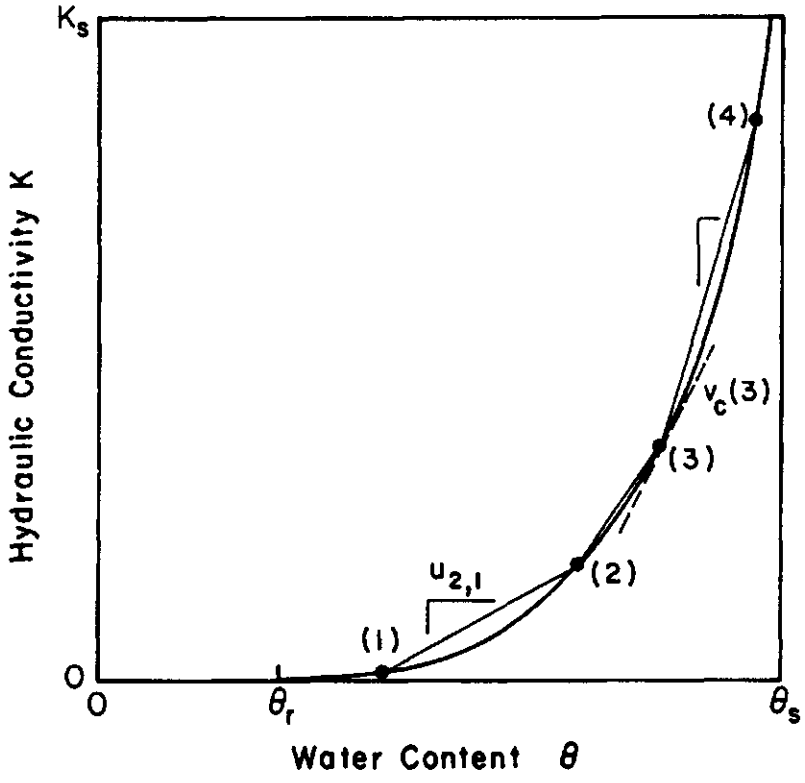

Appendix 11 The analytical calculation of reduced moisture content with depth, integral moisture content with depth, hydraulic conductivity with depth and transmissivity (calculated by taking the integral value of moisture content) with depth

The general idea:

Saturation will occur at depth L_T when the water content just under surface is equal to $\bar{\theta}_0^*$ with $\bar{\theta} \in [0,1]$, i.e. $\bar{\theta}$ is the reduced water content $(\theta - \theta_r)/(\theta_s - \theta_r)$, reaching from 0 till 1.

(11.1) $\bar{\theta} = \bar{\theta}_0^* \quad for\ z = 0$

(11.2) $\bar{\theta} = 1 - (1 - \bar{\theta}_0)\left[\frac{L_T - z}{L_1}\right]^{1/b}$ b>0 $\quad 0 \le z \le L_T$

where L_T = depth of the impermeable or semi impermeable lower boundary, could be a parameter but is set in this study on 1 meter

L_1 = artificial depth of the water table, to be fixed as a parameter

b = parameter to be fitted

for z = L_T $\quad \bar{\theta} = 1$

As soon as the soil starts filling with water a perched water table will rise on the impermeable bedrock. The permeability is presumed to be very high because of the discussed macropores and other structural channels in the rootzone (Beven and Germann, 1982).
We will consider a number of profiles all in the equilibrium stage. This means in the final stage of the equilibrium between gravity and capillary, i.e. no changes will take place if there is no further input of water.

(11.3) $\bar{\theta} = 1 \quad for \quad z \ge z^*$

(11.4) $\bar{\theta} = \left[1 - (1 - \bar{\theta}_0)\left(\frac{z^* - z}{L_1}\right)^{1/b}\right] \qquad z \le z^*$

If in equation (11.4) z = 0, the equation becomes like:

(11.5) $\bar{\theta}_0^* = 1 - (1 - \bar{\theta}_0)\left(\frac{z^*}{L_1}\right)^{1/b}$ $\qquad$ N.B. $z^* \le L_T$

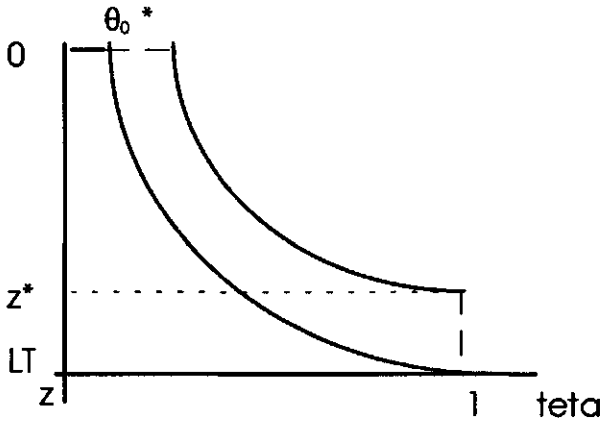

Calculation of the total water content, (Θ dependence on z):

$$\Theta = \int_0^{z^*} \left[1 - \left(\frac{z^* - z}{L_1}\right)^{1/b} \left(1 - \bar{\theta}_0\right)\right] dz + \int_{z^*}^{L_T} 1 dz \qquad (11.6)$$

$$\Theta = \int_0^{L_T} dz - \int_0^{z^*} \left(\frac{z^* - z}{L_1}\right)^{1/b} \left(1 - \bar{\theta}_0\right) dz \qquad (11.6.1)$$

$$\Theta = L_T - \int_0^{z^*} \left(\frac{z^* - z}{L_1}\right)^{1/b} \left(1 - \bar{\theta}_0\right) dz \qquad (11.6.2)$$

Then if: $y = \dfrac{z^* - z}{L_1}$ and $z = z^* - L_1 y$ and $dz = -L_1 dy$, we can write:

$$\Theta = L_T - \int_0^{z^*/L_1} \left(1 - \bar{\theta}_0\right) L_1 y^{1/b} \, dy \qquad (11.7)$$

$$\Theta = L_T - \left[\left(1 - \bar{\theta}_0\right) L_1 \frac{b}{b+1} \left(\frac{z^*}{L_1}\right)^{\frac{b+1}{b}}\right] \qquad (11.7.1)$$

$$\Theta = L_T \left[1 - \left(1 - \bar{\theta}_0\right) \frac{L_1}{L_T} \quad \frac{b}{b+1} \left(\frac{z^*}{L_1}\right)^{\frac{b+1}{b}}\right] \qquad (11.7.2)$$

Starting from the previous relationship we can find $\dfrac{z^*}{L_1}$ as a function of Θ

(11.8) $$\frac{z^*}{L_1} = \left[\frac{L_T - \Theta}{(1-\bar{\theta}_0)L_1} \quad \frac{b+1}{b} \right]^{\frac{b}{b+1}}$$

With the limits (minimum and maximum values) of:

$$z^* = L_T \quad \Rightarrow \quad \Theta = L_T \left[1 - (1-\bar{\theta}_0) \left(\frac{L_T}{L_1} \right)^{1/b} \frac{b}{b+1} \right]$$

$$z^* = 0 \quad \Rightarrow \quad \Theta = L_T$$

Permeability in relation with θ , (hydraulic conductivity (K) depending on moisture content):

(11.9) $$K(\bar{\theta}) = K_s \left[1 - (1-\bar{\theta})^{1/c} \right] \qquad c > 0$$

(11.9.1) $$z \geq z^* \quad \Rightarrow \quad K(\bar{\theta}) = K_s$$

(11.9.2) $$z \leq z^* \quad \Rightarrow \quad K(\bar{\theta}) = K_s \left[1 - (1-\bar{\theta}_0)^{1/c} \left(\frac{z^* - z}{L_1} \right)^{1/bc} \right]$$

The horizontal transmissivity of the layer can be found by integration along the depth L_T:

(11.10) $$T = \int_0^{z^*} K_s \left[1 - (1-\bar{\theta}_0)^{1/c} \left(\frac{z^* - z}{L_1} \right)^{1/bc} \right] dz + \int_{z^*}^{L_T} K_s \, dz$$

(11.10.1) $$T = \int_0^{L_T} K_s \, dz - \int_0^{z^*} K_s \, (1-\bar{\theta}_0)^{1/c} \left(\frac{z^* - z}{L_1} \right)^{1/bc} dz$$

(11.10.2) $$T = K_s \, L_T - K_s \, (1-\bar{\theta}_0)^{1/c} \int_0^{z^*} \left(\frac{z^* - z}{L_1} \right)^{1/bc} dz$$

then if $y = \frac{z^* - z}{L_1}$ and $z = z^* - L_1 y$ and $dz = -L_1 dy$ $\begin{cases} z = 0 & y = \frac{z^*}{L_1} \\ z = z^* & y = 0 \end{cases}$

$$(11.11) \qquad T = K_s L_T - K_s L_1 \left(1 - \bar{\theta}_0\right)^{1/c} \int_0^{z^*/L_1} y^{1/bc}\, dy$$

$$(11.11.1) \qquad T = K_s L_T - K_s L_1 \left(1 - \bar{\theta}_0\right)^{1/c} \frac{bc}{bc+1} \left(\frac{z^*}{L_1}\right)^{\frac{bc+1}{bc}}$$

$$(11.11.2) \qquad T = K_s L_T \left[1 - \frac{L_1}{L_T}\left(1 - \bar{\theta}_0\right)^{1/c} \frac{bc}{bc+1} \left(\frac{z^*}{L_1}\right)^{\frac{bc+1}{bc}}\right]$$

The value of $\frac{z^*}{L_1}$ as in equation (11.8) can be substituted into a transmissivity expression so as to give transmissivity as a function of total water content.

$$(11.12) \quad T = K_s L_T \left[1 - \frac{L_1}{L_T}\left(1 - \bar{\theta}_0\right)^{1/c} \frac{bc}{bc+1} \left(\frac{L_T - \Theta}{\left(1 - \bar{\theta}_0\right) L_1} \frac{b+1}{b}\right)^{\frac{bc+1}{c(b+1)}}\right]$$

$$(11.12.1) \quad T = K_s L_T \left[1 - \frac{L_1}{L_T}\left(1 - \bar{\theta}_0\right)^{\frac{b(1-c)}{c(b+1)}} \frac{bc}{bc+1} \left(\frac{b+1}{b}\right)^{\frac{bc+1}{c(b+1)}} \left(\frac{L_T - \Theta}{L_1}\right)^{\frac{bc+1}{c(b+1)}}\right]$$

$$(11.12.2) \quad T = K_s L_T \left[1 - \left(\frac{L_1}{L_T}\right)^{\frac{c-1}{c(b+1)}} \frac{bc}{bc+1} \left(1 - \bar{\theta}_0\right)^{\frac{b(1-c)}{c(b+1)}} \left(\frac{b+1}{b}\right)^{\frac{bc+1}{c(b+1)}} \left(1 - \frac{\Theta}{L_T}\right)^{\frac{bc+1}{c(b+1)}}\right]$$

The relationship holds for the minimum and maximum values of Θ ranging from:

$$\Theta \in \left[L_T \left(1 - \left(1 - \bar{\theta}_0\right)\left(\frac{L_T}{L_1}\right)^{1/b} \left(\frac{b}{b+1}\right)\right),\ L_T\right]$$

This transmissivity equation (11.12.2) is similar to that of the conductivity equation mentioned in eq.(11.9) in relation with θ.
We can therefore rewrite (11.12.2) as:

$$(11.13)\, T = K_s\, L_T \left[1 - \alpha \left(1 - \frac{\Theta}{L_T} \right)^{\beta} \right]$$

With

$$\alpha = \left(\frac{L_1}{L_T} \right)^{\frac{c-1}{c\,(b+1)}} \frac{bc}{bc+1} \left(1 - \overline{\theta}_0 \right)^{\frac{b\,(1-c)}{c\,(b+1)}} \left(\frac{b+1}{b} \right)^{\frac{bc+1}{c\,(b+1)}}$$

and

$$\beta = \frac{bc+1}{c(b+1)}$$

Appendix 12 First twelve profiles. With higher moisture content at the bottom than at the top. Transition-phase from 0.5 till 0.75 m. below surface

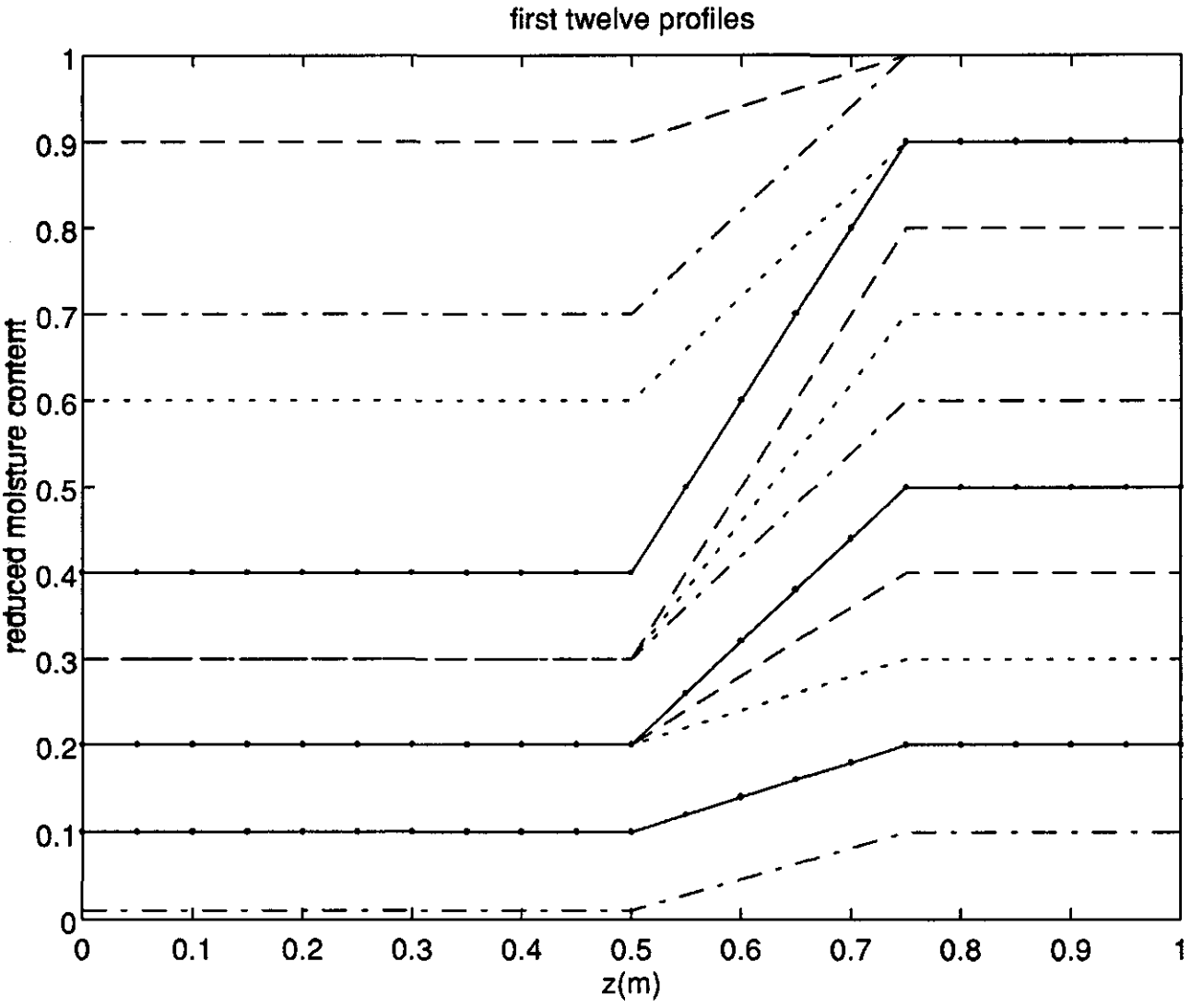

Appendix 13 Second twelve profiles. With changed transition form from 0.5 till 0.7 or 0.75 m.

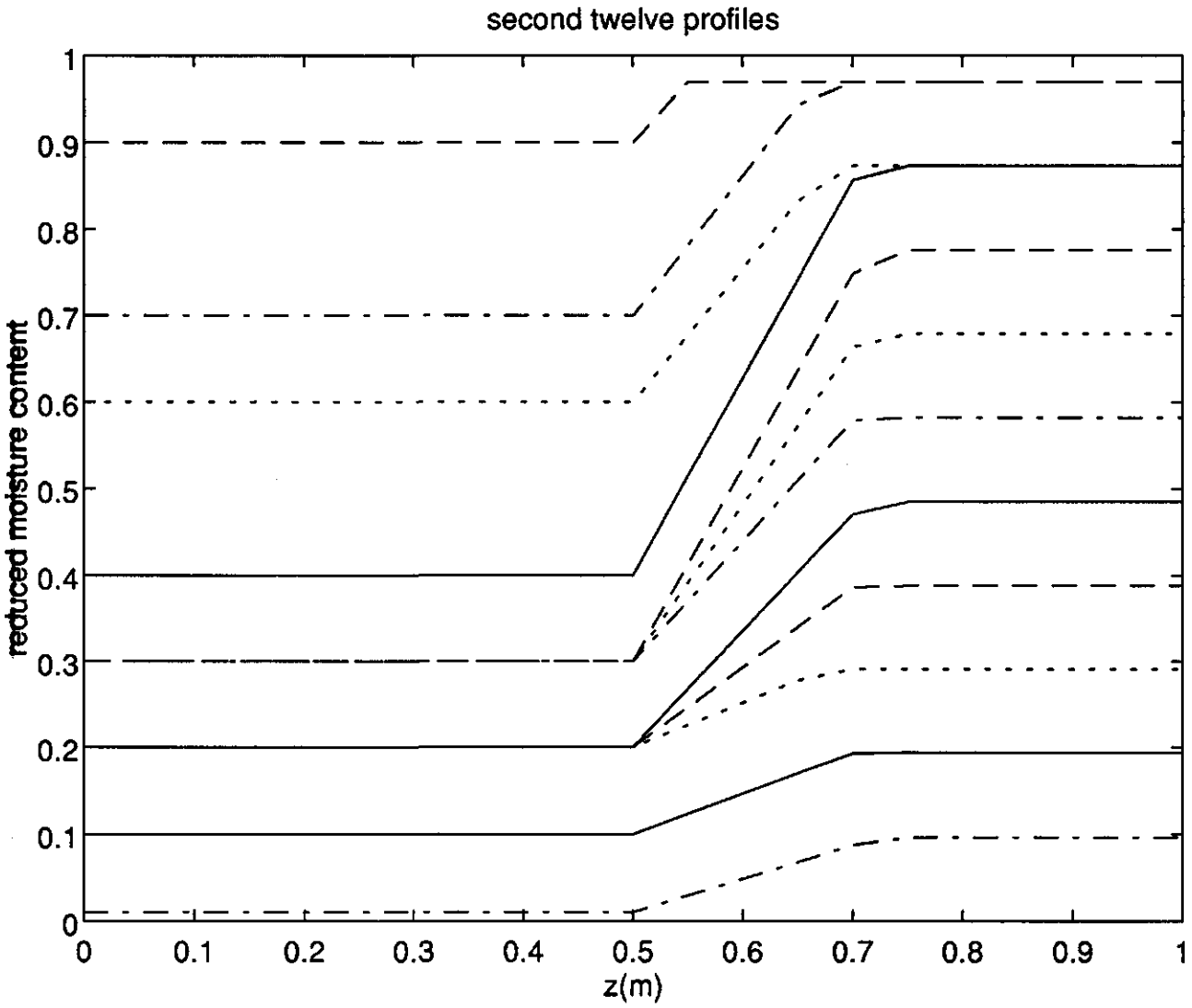

Appendix 14 Third twelve profiles with lower moisture content at the bottom than at the top (reverse profiles from appendix 12). Transition from 0.25 till 0.50 m. below surface

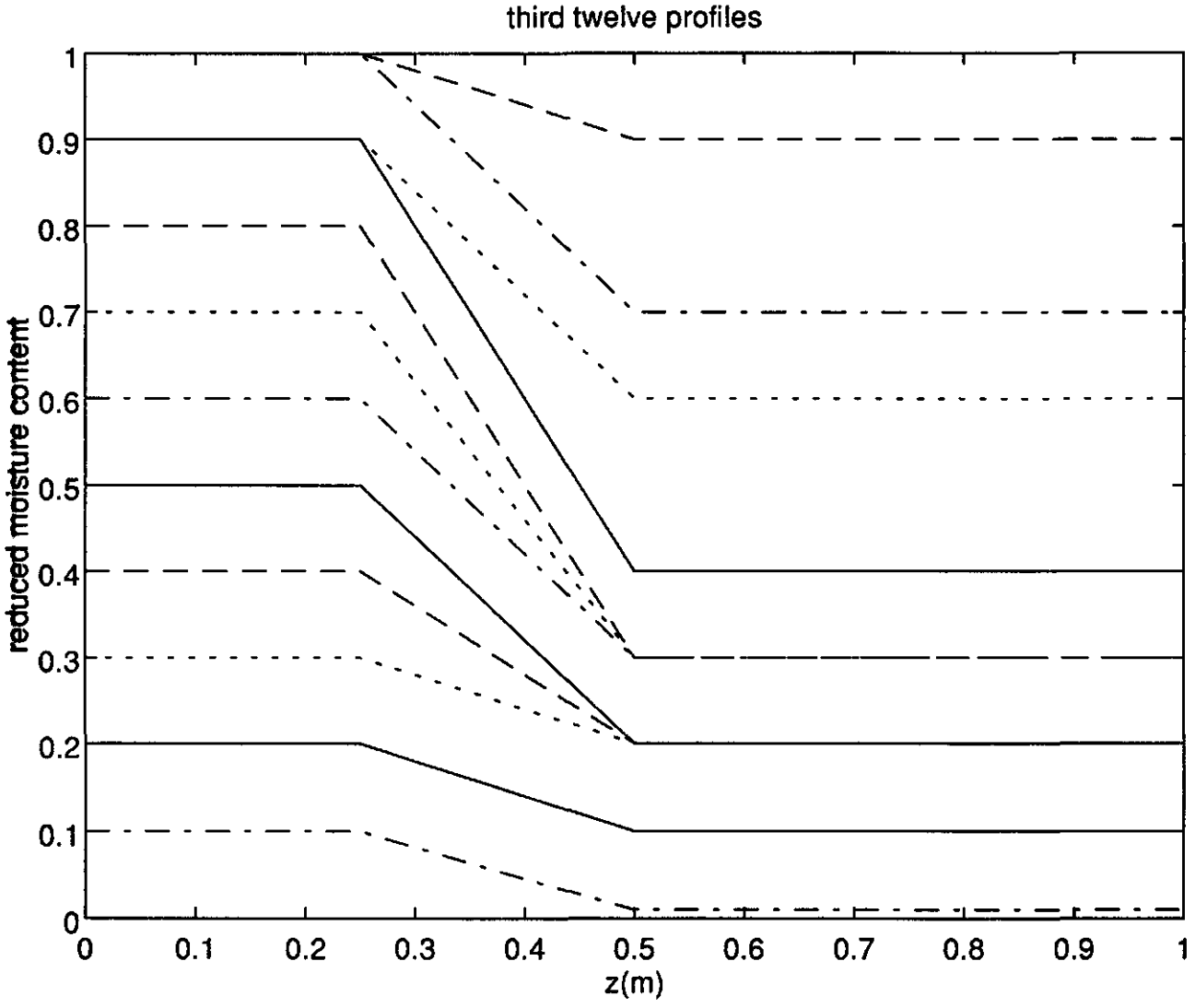

Appendix 15 Fourth twelve profiles with varied forms of transition phase from 0 till 0.75 m.

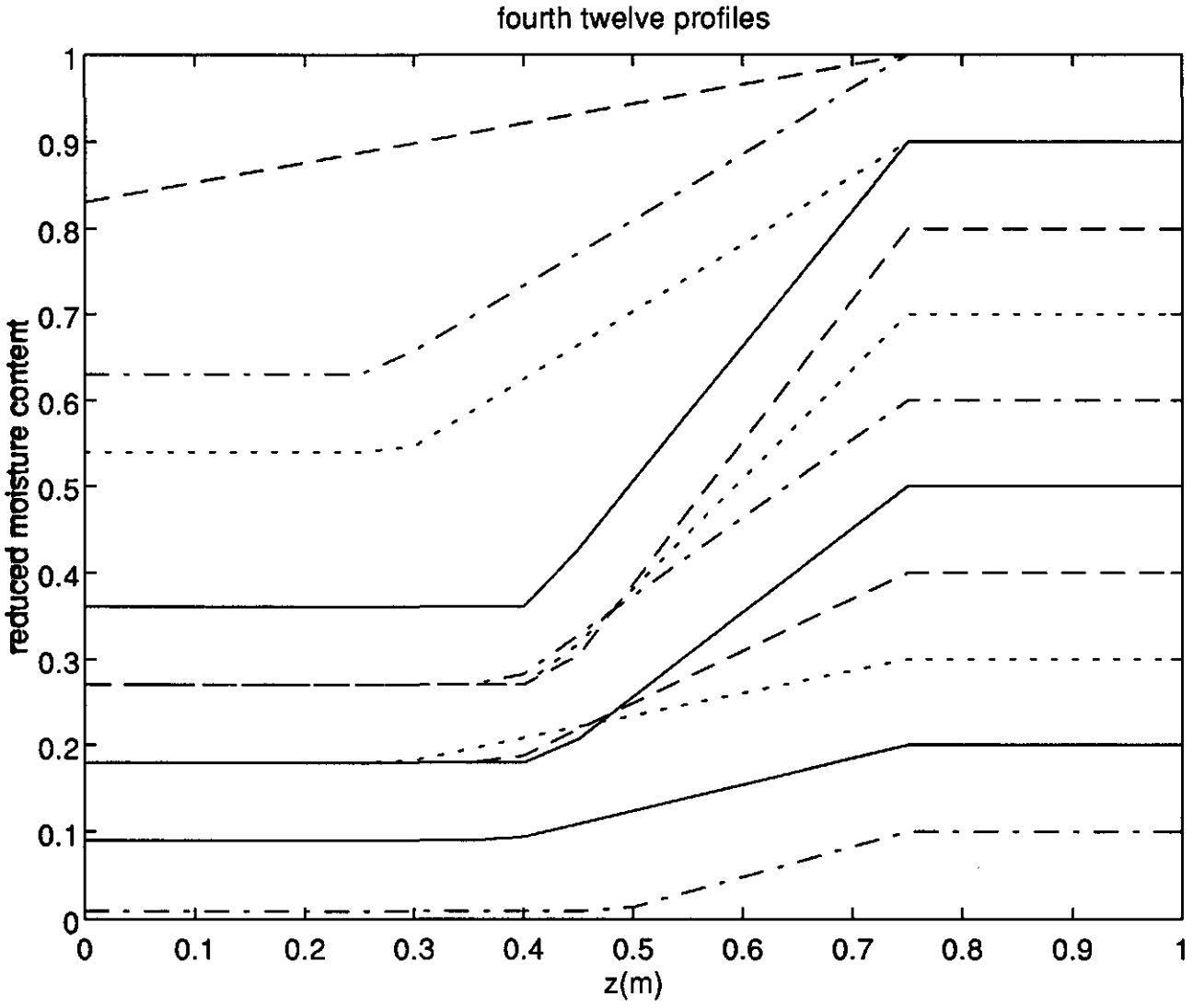

Appendix 16 Ten extra profiles with an extreme low moisture content at the top of the profile and a high moisture content at the bottom of the profile. Transition is varying from 0.1 till .0.75 m. below surface.

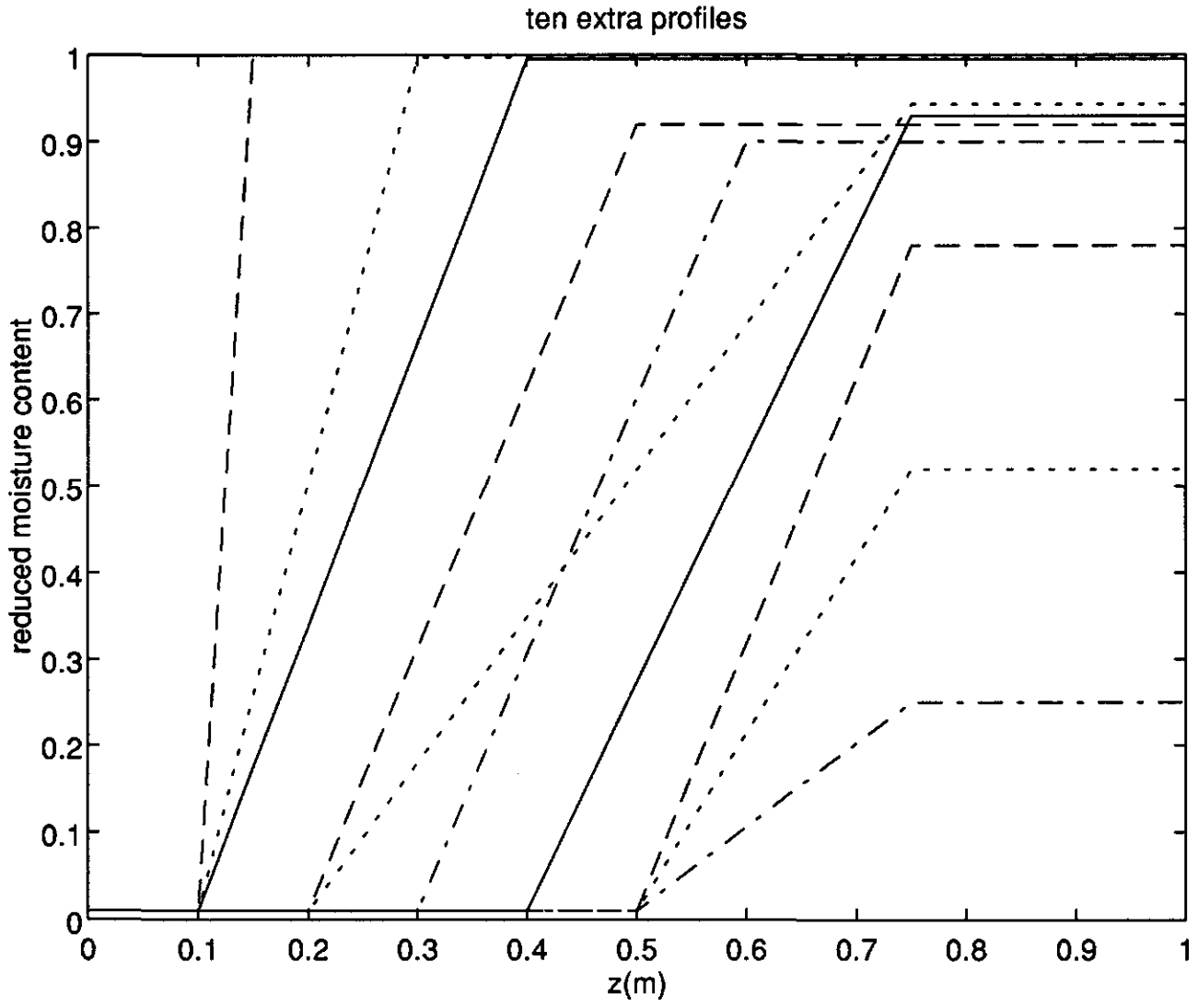

Appendix 17 Compared flux index calculated with point by point moisture content or average moisture content

+ = presenting appendix 12
. = presenting appendix 13
o = presenting appendix 14 (note that this is the same as appendix 12)
x = presenting appendix 15
* = presenting appendix 16
— = presenting the calculation of flux index with the average moisture content

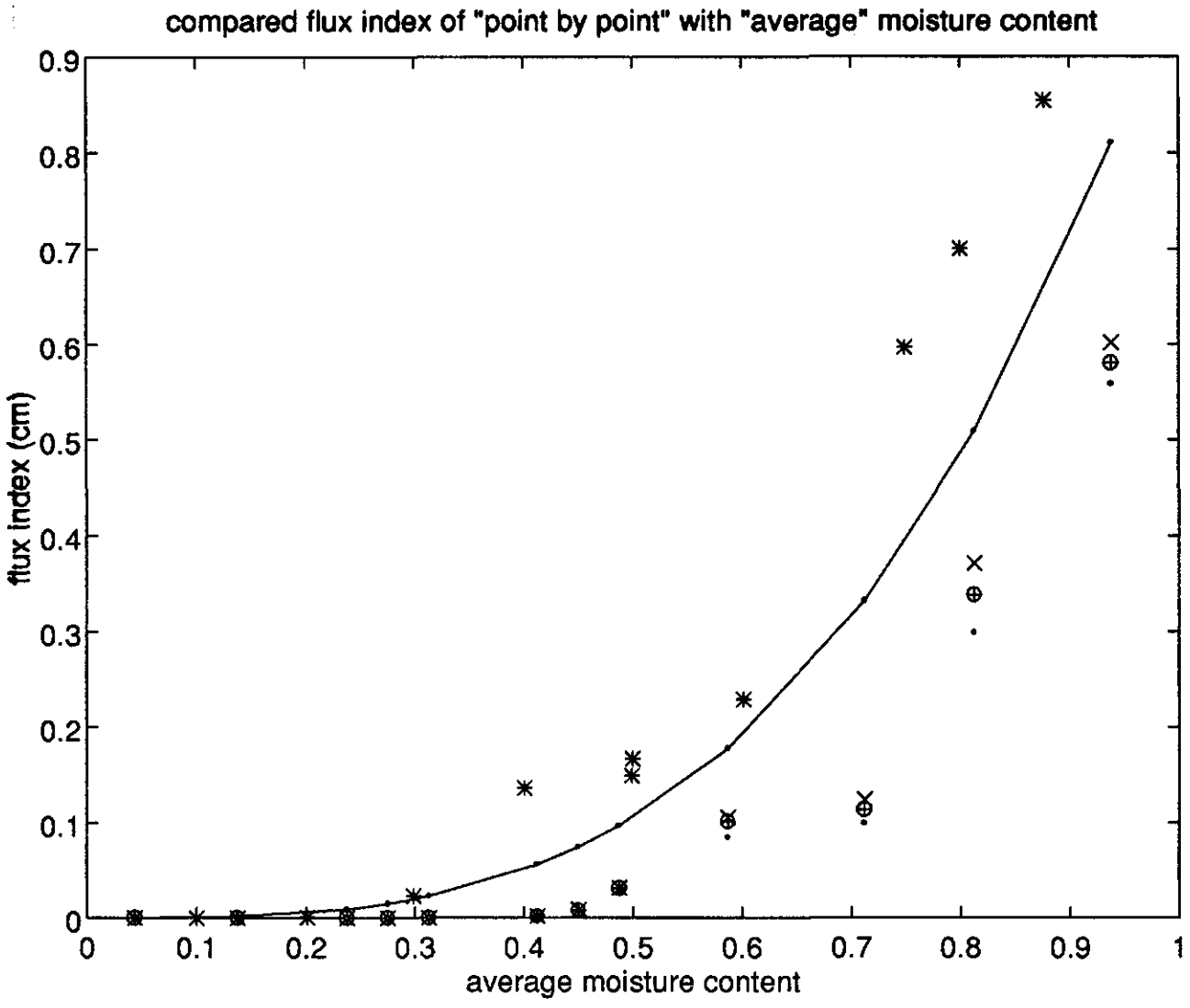

Appendix 18 Relation of reduced moisture content with depth calculated with van Genuchten equation (5.3) represented by (-.-.) and our equation (11.4) represented by (—)

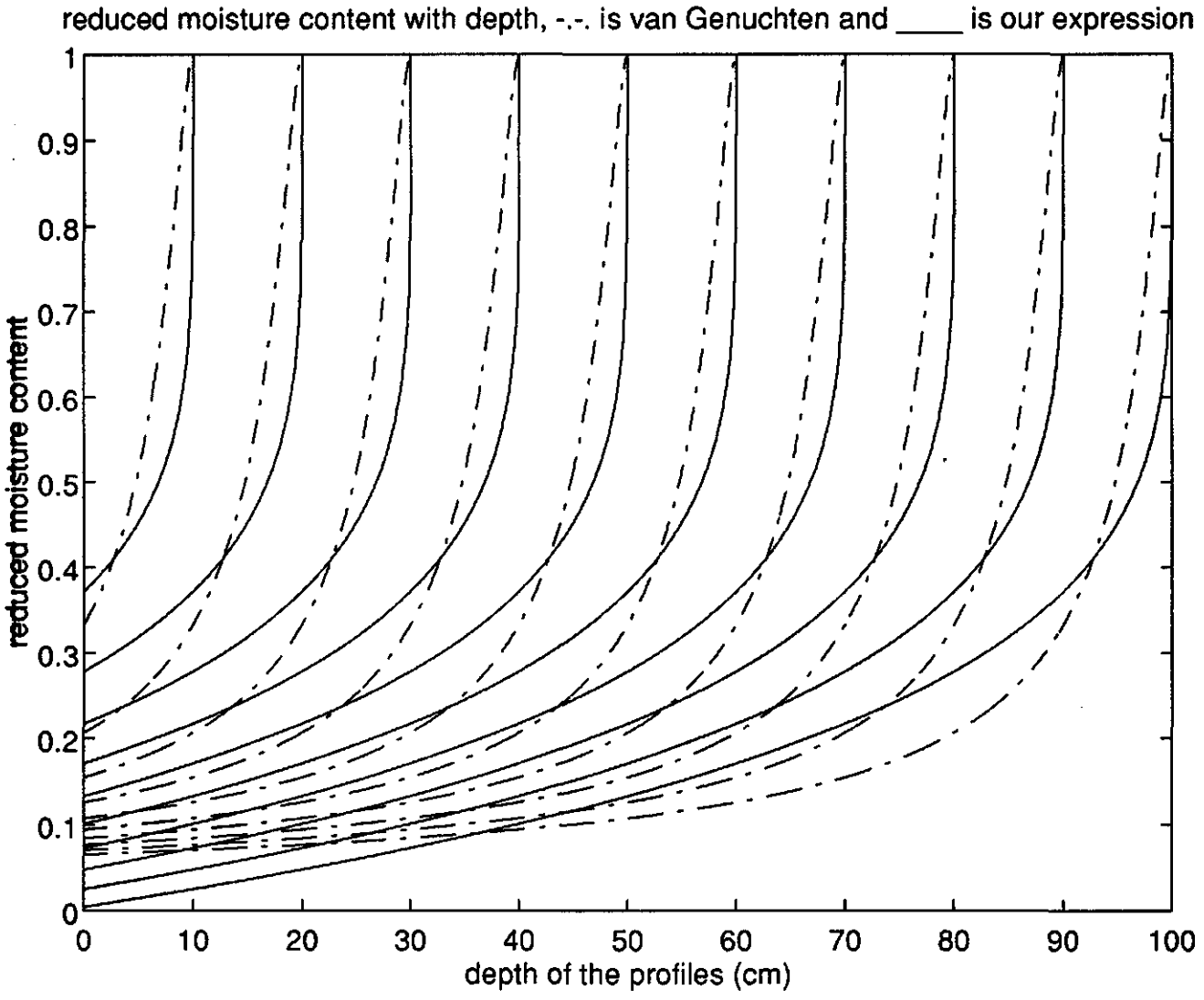

Appendix 19 Percentage of soil filled with water calculated with van Genuchten equation (5.3) represented by (x), compared with our equation (11.7.2) represented by (0)

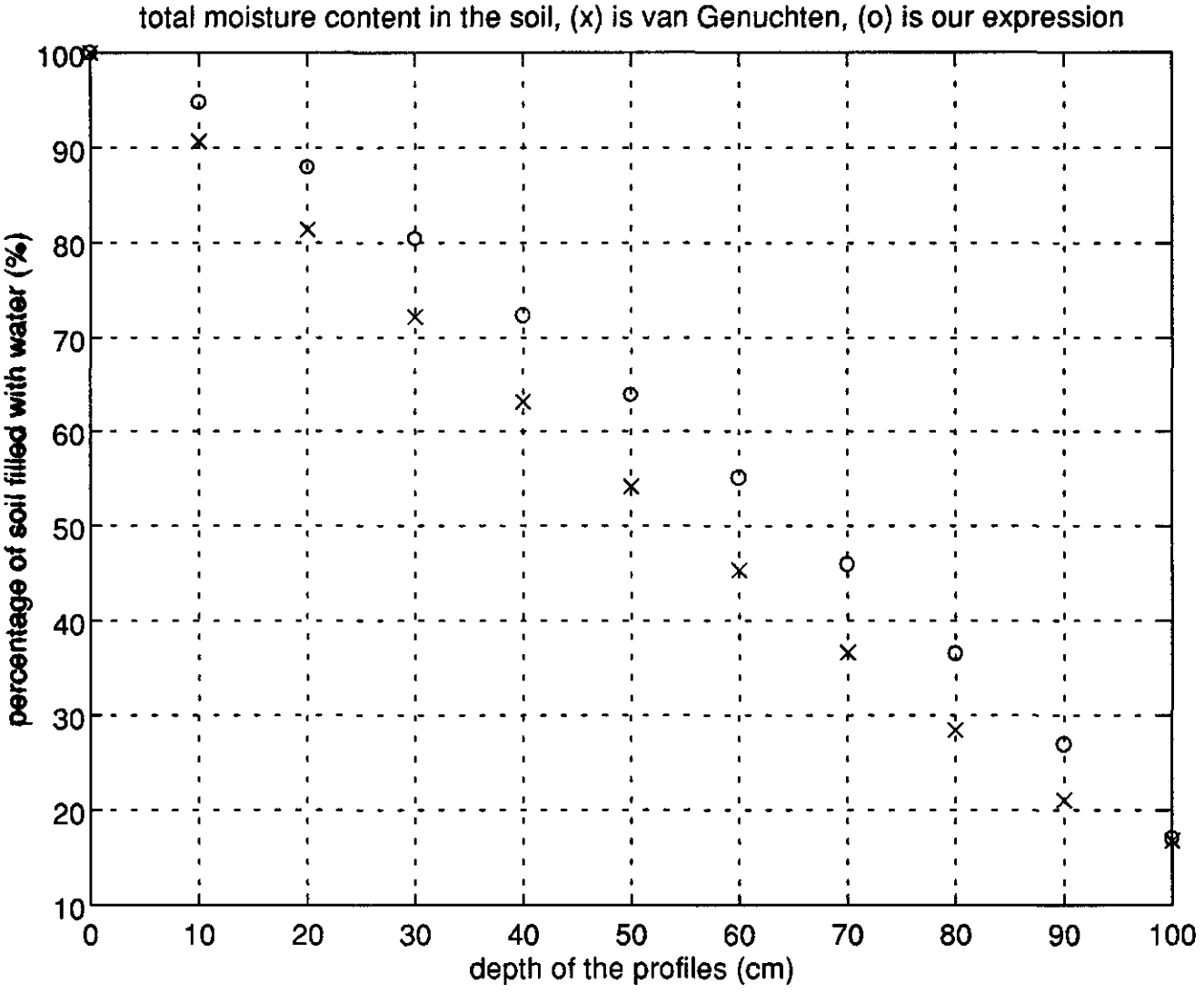

Appendix 20 Relation of hydraulic conductivity with depth calculated with van Genuchten equation (5.6) represented by (-.-.) and our equation (11.9) represented by (—)

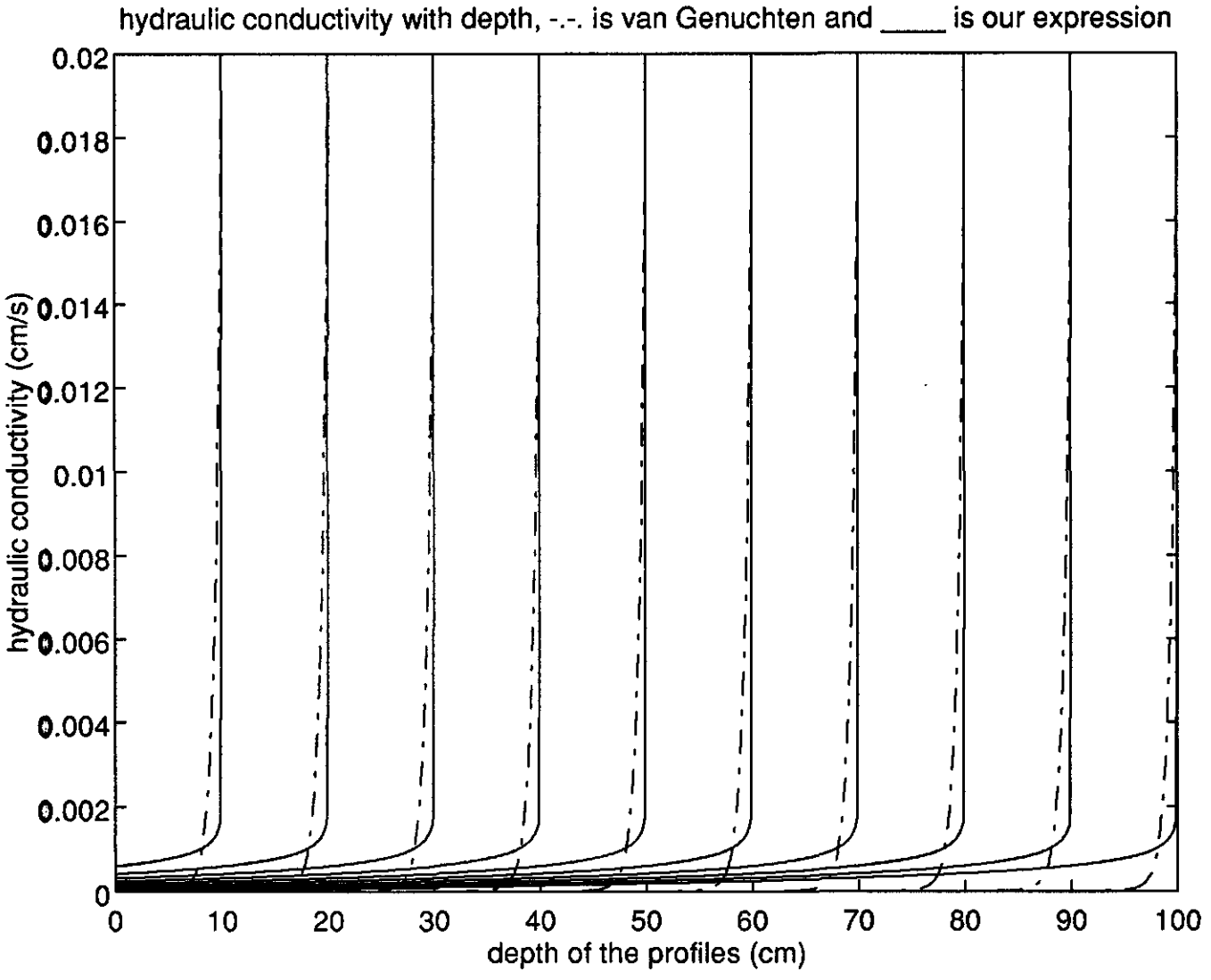

Appendix 21 Transmissivity calculated with van Genuchten equation (5.6) represented by (x), compared with transmissivity calculated with our equation (11.13) represented by (o)

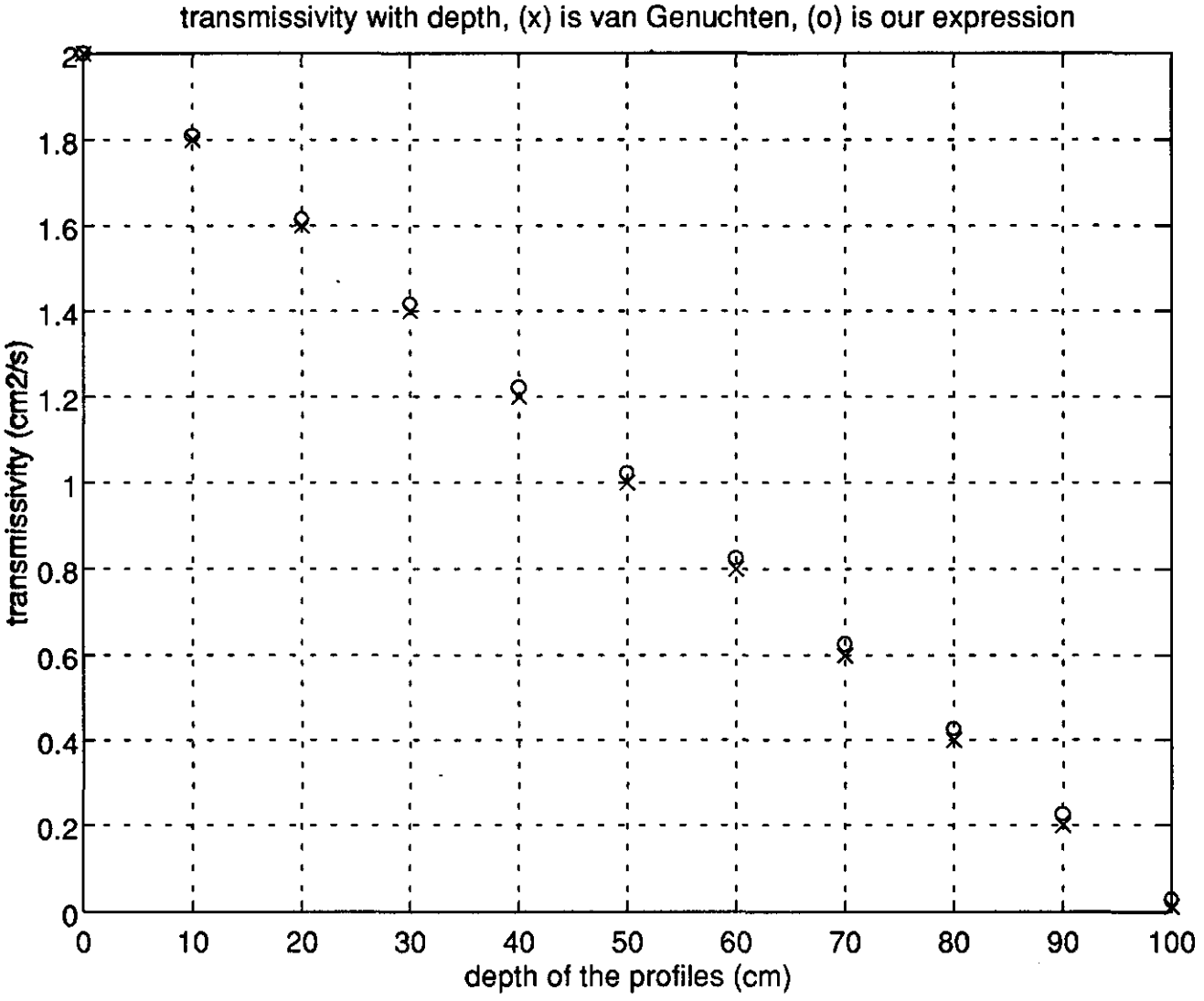

Appendix 22 Increasing transmissivity with increasing moisture content calculated with van Genuchten equations (5.3) and (5.6) represented by -.-. and calculated with our equations (11.7.2) and (11.3) represented by —

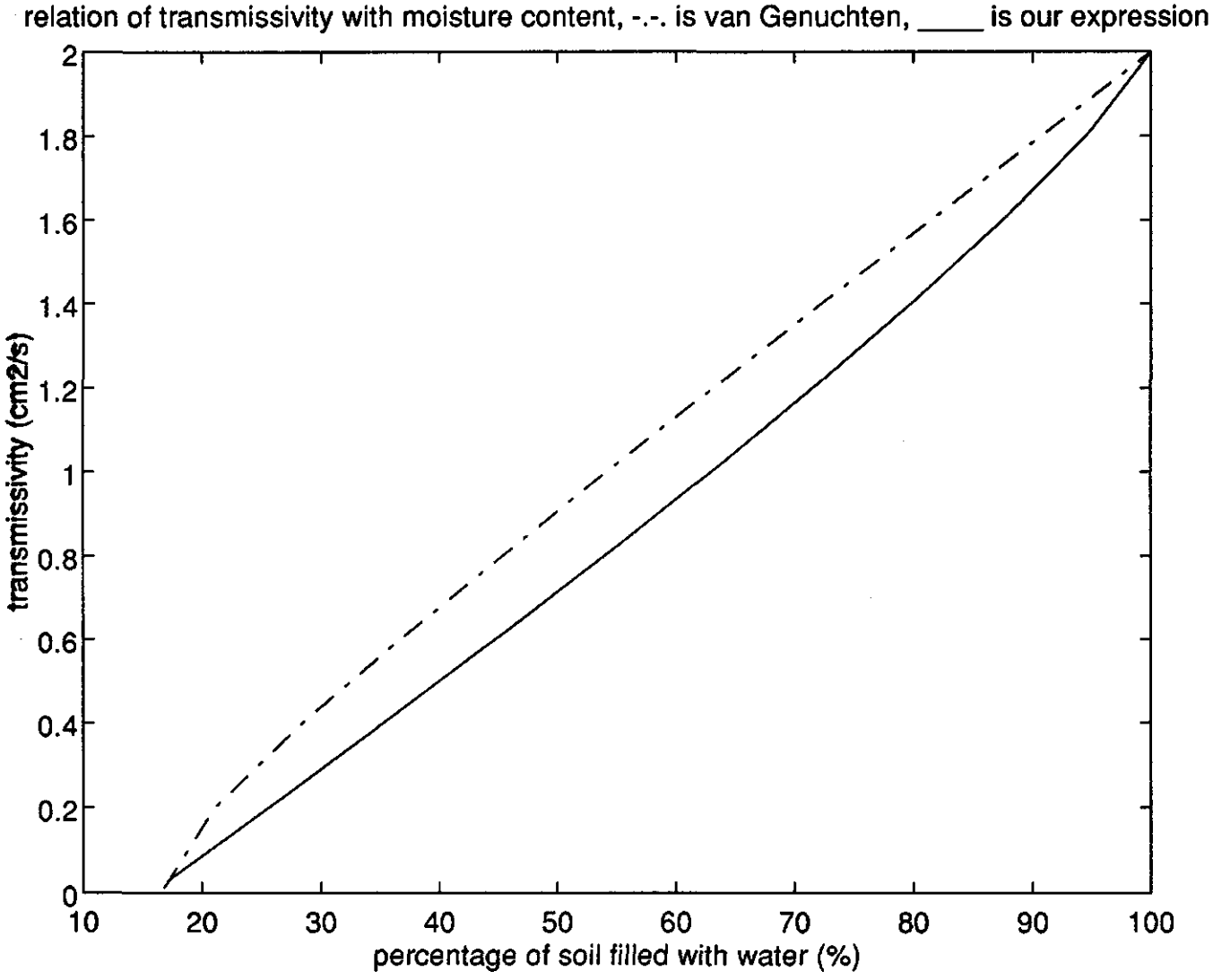

Table 1 The explained variance (EV), the determination coefficient (DC) and the correlation coefficient (CC) of both calibration period (February till May 1990) and validation period (June till December 1990). See TOPMODEL results in appendix 8 and appendix 9.

EV Calibration	EV Validation	DC Calibration	DC Validation	CC Calibration	CC Validation
0.8795	0.7234	0.8782	0.7030	0.9371	0.8385

The mathematical definitions of the evaluation coefficients are the following :

$$EV = 1 - \frac{\sum_{i=1}^{i=n} (\varepsilon_i - \mu_\varepsilon)^2}{\sum_{i=1}^{i=n} (Qr_i - \mu_r)^2} \quad \text{(explained variance)}$$

$$DC = 1 - \frac{\sum_{i=1}^{i=n} \varepsilon_i^2}{\sum_{i=1}^{i=n} (Qr_i - \mu_r)^2} \quad \text{(determination coefficient)}$$

$$CC = \sqrt{DC} \quad \text{(correlation coefficient)}$$

where n = number of point used for the calculation
ε = error Qr-Qs
Qr = recorded discharge
Qs = simulated discharge
μ_ε = mean of the error
μ_r = mean of the recorded discharges

Table 2 Soil-level water balance component (TOPMODEL). Obtained parameter values of both calibration period (February till May 1990) and validation period (June till December 1990). See TOPMODEL results in appendix 8 and appendix 9.

PARAMETER	PHYSICAL MEANING	OBTAINED VALUE
m	Exponential decay rate of Transmissivity with depth	0.016 (m)
Sko	Hydraulic conductivity of the soil	200 (m/hr.)
Srmax	Root zone storage	0.004 (m)
Inter	Interception	0.00005 (m) (given value)

Table 3.1 Calibrated values of parameters used to fit equation (6.6), as shown in appendix 17

	Character	Estimated value
parameter in eq. (6.6)	*c1*	3.25
parameter in eq. (6.6)	*c2*	10

Table 3.2 Calibrated values of parameters and soil characteristics used to fit van Genuchten equations with our equations as shown in appendices 18 till 22

Parameter meaning	Character	Estimated value
artificial depth of the water-talble	L_1	54 cm.
parameter in eq. (5.7)	b	5
initial reduced moisture content	$\bar{\theta}_0$	0.12
saturated hydraulic conductivity	K_s	0.02 cm/s
parameter in eq. (5.8)	c	15
real saturated moisture content	θ_s	0.40
real residual moisture content	θ_r	0.05
parameter in eq. (5.3)	α	0.44
parameter in eq. (5.3)	n	1.72
parameter in eq. (5.3)	m	0.4186 (N.B. $m=1-1/n$)
parameter in eq. (5.6)	LL	2.5